1980

Seismicity and gravity studies of faulting in the Kalispell Valley northwest Montana

Michael C. Stickney
The University of Montana

SEISMICITY AND GRAVITY STUDIES OF FAULTING IN THE KALISPELL VALLEY, NORTHWEST MONTANA

by

Michael C. Stickney

B.S., University of Montana, 1978

Presented in partial fulfillment of the requirements for the degree of

Master of Science

UNIVERSITY OF MONTANA

1980

Approved by:

Chairman, Board of Examiners

Dean, Graduate School

6/3/80

Date

ProQuest LLC.
789 East Eisenhower Parkway
P.O. Box 1346
Ann Arbor, MI 48106 - 1346

ABSTRACT

Stickney, Michael C., M.S., Spring, 1980 Geology

Seismicity and Gravity Studies of Faulting in the Kalispell Valley, Northwest Montana

Director: Dr. Anthony Qamar

The Kalispell Valley forms part of the Rocky Mountain Trench in northwest Montana. Numerous earthquakes have occurred within the Kalispell Valley and represent the northernmost seismicity along the Intermountain Seismic Belt. Gravity data indicates that normal faults bound the Kalispell Valley and the northern Mission Range. P-wave first motions from the February 4, 1975 Kalispell Valley earthquake (M_L = 5.0) indicate oblique-slip at the northern end of the Mission Range on a fault trending northeast across the valley. Gravity data and seismicity suggest that the floor of the Kalispell Valley is moving downward and tilting eastward with respect to the Mission Range. In the southwest corner of the Kalispell Valley, vertical movement along faults may slightly tilt the surface of the Kalispell Valley and affect the course and gradient of the Flathead River.

ACKNOWLEDGMENTS

I thank the members of my thesis committee, Dr. Anthony Qamar, Dr. David Alt, and Dr. Wayne Van Meter for their discussions and critical suggestions. I also thank Dr. Johnnie Moore for his interesting discussions and John Cuplin for his suggestions and assistance with the figures. Finally, I thank the past and present employees, and the other resident of the Earthquake Research Lab (WRH), for enduring me and my messes.

TABLE OF CONTENTS

LIST OF FIGURES

LIST OF TABLES

CHAPTER I

INTRODUCTION

Regional Setting

The Kalispell Valley lies in the Rocky Mountains of northwestern Montana and is part of a succession of valleys which extend to the northwest across British Columbia to form the Rocky Mountain Trench. Daly (1912) described it as "a long narrow intermountain depression". Previous workers (Daly, 1912; Schofield, 1921; Leech, 1959; Garland and others, 1961; Thompson, 1962; and Mudge, 1970) believe that steeply-dipping, northwest-trending normal faults bound one or both sides of the trench along its southern half. Gravity data from the Kalispell Valley and British Columbia (Garland and others, 1961; and Thompson, 1962) suggest that northeast-trending faults cut across the Rocky Mountain Trench. To the south, the Kalispell Valley splits, southeastward into the Swan Valley and southward into the Flathead Valley (see Fig. 1). The Mission Range separates the Swan and Flathead valleys. Elevations of the peaks in the southern Missions exceed 3000 meters; the elevations decrease steadily northward until bedrock disappears beneath Cenozoic deposits in the Kalispell Valley.

Earthquakes in the Kalispell Valley indicate continued movement along some faults. The earthquakes in northwest Montana represent the northernmost seismicity along the Intermountain Seismic Belt, an

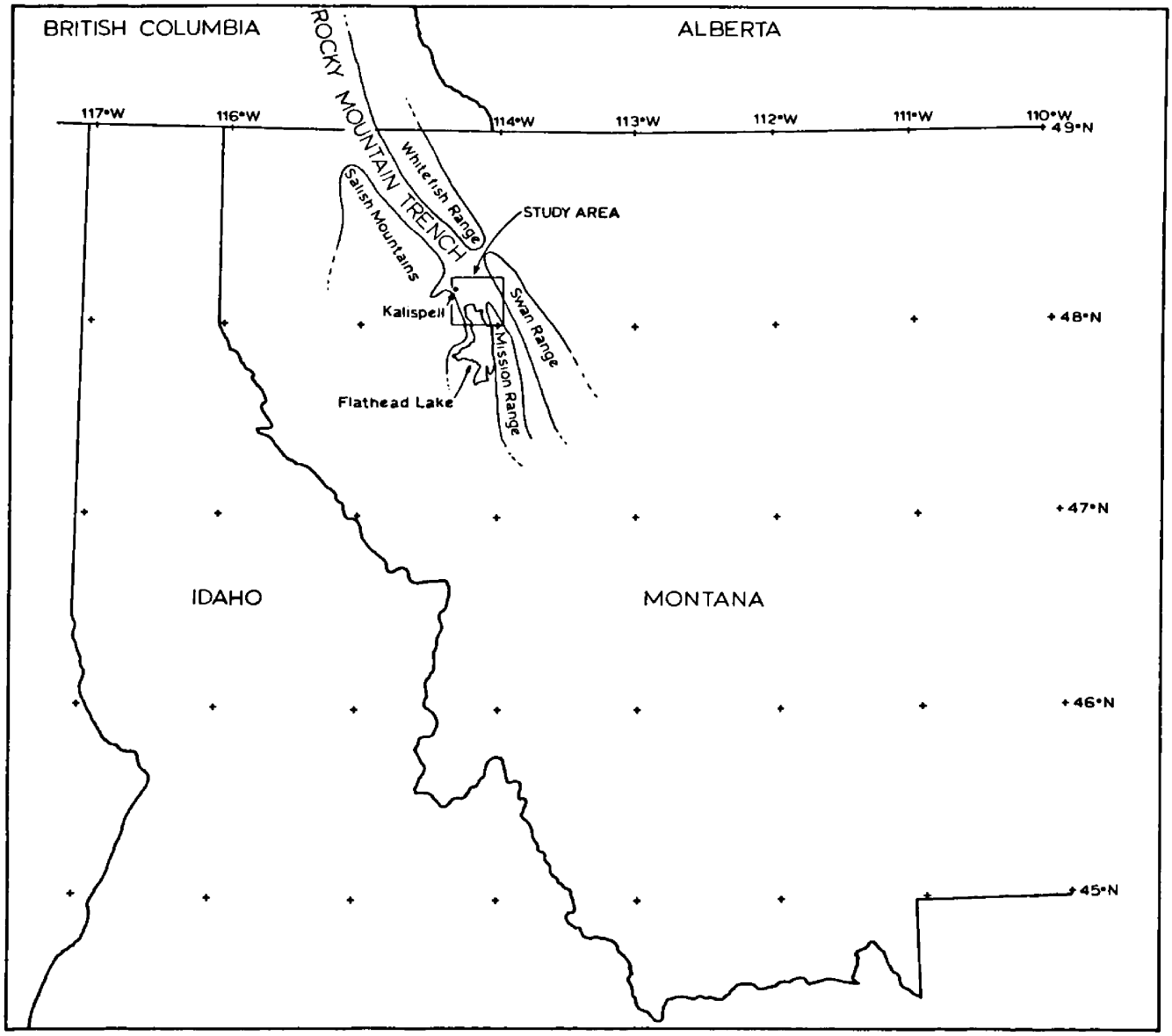

Figure 1. Location map showing the study area and surrounding features.

arcuate zone of seismicity extending from Nevada northward through Utah, Wyoming, Idaho and into northwest Montana where it apparently ends (Smith and Sbar, 1974). The moderate level of seismicity contrasts with low seismicity levels along the Rocky Mountain Trench in southern British Columbia (Milne, 1966; and Milne and Davenport, 1969).

Methods of Study

I conducted a gravity survey in the southern Kalispell Valley to determine the bedrock configuration beneath the Cenozoic deposits. From the gravity data, one can estimate the trend and displacement of buried faults. I also operated temporary networks of seismograph stations to collect data from minor earthquakes in the Kalispell Valley area. Information from the temporary seismograph networks supplements data from about 100 Kalispell Valley earthquakes recorded by the University of Montana Earthquake Research Lab. Careful study of these earthquake indicate movement along several faults identified from gravity data and provides information about the present-day tectonics.

Maps showing recently active faults in western Montana (Pardee, 1950; and Witkind, 1975) do not show active faults in the Kalispell Valley area. However, geology mapped by Johns (1970) indicates significant displacement along normal faults in the area during Cenozoic time. A brief visit to the field with D. Winston verified the existence of old northeast-trending faults in the Swan Range.

CHAPTER II

GRAVITY SURVEY OF THE SOUTHERN KALISPELL VALLEY

Gravity Data Collection

From August 29 to September 9, 1979, I measured the acceleration of gravity at 285 locations (stations) in the southern Kalispell Valley using a Worden gravimeter. Gravity readings were taken at section corners, road intersections, bench marks or any other location with an elevation marked on the U.S.G.S. 7 1/2 minute topographic maps which covered the area. Accurate elevations for seven gravity stations could not be determined from the maps, so elevations were surveyed in from the nearest point of known elevation using a Nikon theodolite. The survey covered approximately 370 square kilometers with an average station density of 0.75 stations per square kilometer. The lowest station density exists along the foot of the Swan Range in the eastern Kalispell Valley because of limited access and few marked elevations. For similar reasons, no readings were taken in the Swan Mountains. Readings taken at one of three base stations every two hours allowed me to plot a drift curve for each day of the gravity survey. The three base stations were tied together by going from one base station to another and then back to the first, taking a reading at each. In this manner, the differences in the acceleration of gravity at the three base stations were determined to

within 0.05 milligals. An additional reading taken at the Kalispell Airport, a point of known absolute gravity, allowed me to calculate the absolute gravity at all 285 gravity stations.

Gravity Data Reduction

Daily drift curves, prepared by the method described in Dobrin (1960), of gravity at base stations were used to remove instrument and tidal fluctuations. Appendix 1 lists the latitude, longitude, elevation and terrain corrections used to compute free air and Bouguer gravity anomalies for each station. Appendix 2 contains a listing of the Fortran program BOUGER.FOR, the program used to calculate the Bouguer gravity anomalies. The terrain corrections were determined in two parts. A Hammer chart and terrain correction table (Bible, 1962) allowed estimation of gravity effect due to surrounding terrain out to a distance of 895 meters (through the F ring) from each gravity station. The U.S. Geological Survey in Denver computed the gravity effect of terrain from 895 meters to a distance of 160 kilometers from each station using terrain elevations digitized from 1:250,000 scale maps at intervals of about 1 kilometer. The two terrain corrections for each station were added together to obtain the total terrain correction. A density of 2.67 grams per cubic centimeter (the usual assumed density of average crustal rocks) was assumed when computing all terrain corrections. The maximum terrain correction computed is 3.0 milligals; the average value is about 0.7 milligals. The data were gathered and reduced carefully enough to attain a precision of

at least 0.5 milligals relative to the Kalispell Airport value of 980581.9 milligals (Woollard, 1958). The largest source of error comes from uncertainty of the gravity station elevations. A one foot elevation error will affect the gravity reading at a station by about 0.06 milligals (combined elevation and Bouguer correction).

The Bouguer Gravity Map

General features of the Bouguer gravity map, shown in Figure 2, include a prominent NNW trending gravity high which decreases in a stair-step fashion to the northwest where it ends near the center of the map. A northeast-southwest striking gravity gradient traverses the Kalispell Valley for three quarters of its width and marks the northern end of the gravity high. A gravity low centered north of the map area and along the eastern half of the Kalispell Valley, lies north of the transverse gravity gradient. Gravity contours along the southwest side of the valley roughly parallel the bedrock outcrop and decrease in value with increasing distance from bedrock. The -130 milligal contour surrounds all of the bedrock outcrops along the southwest side of the valley and most of the bedrock outcrop at the northern end of the Mission Range. A northwest-trending, trough-shaped gravity low with about six milligals of relief separates the gravity high associated with the northern end of the Mission Range from the gravity high paralleling the southwest valley edge. The final major gravity feature shown by this map consists of a large gravity low centered southeast of the map area in the northern end of the Swan

Figure 2. Complete Bouguer gravity anomaly map of the southern Kalispell Valley. Contour interval is 2.0 milligals. Cross sections shown in Figures 4, 5 and 7. Gravity data listed in Appendix 1.

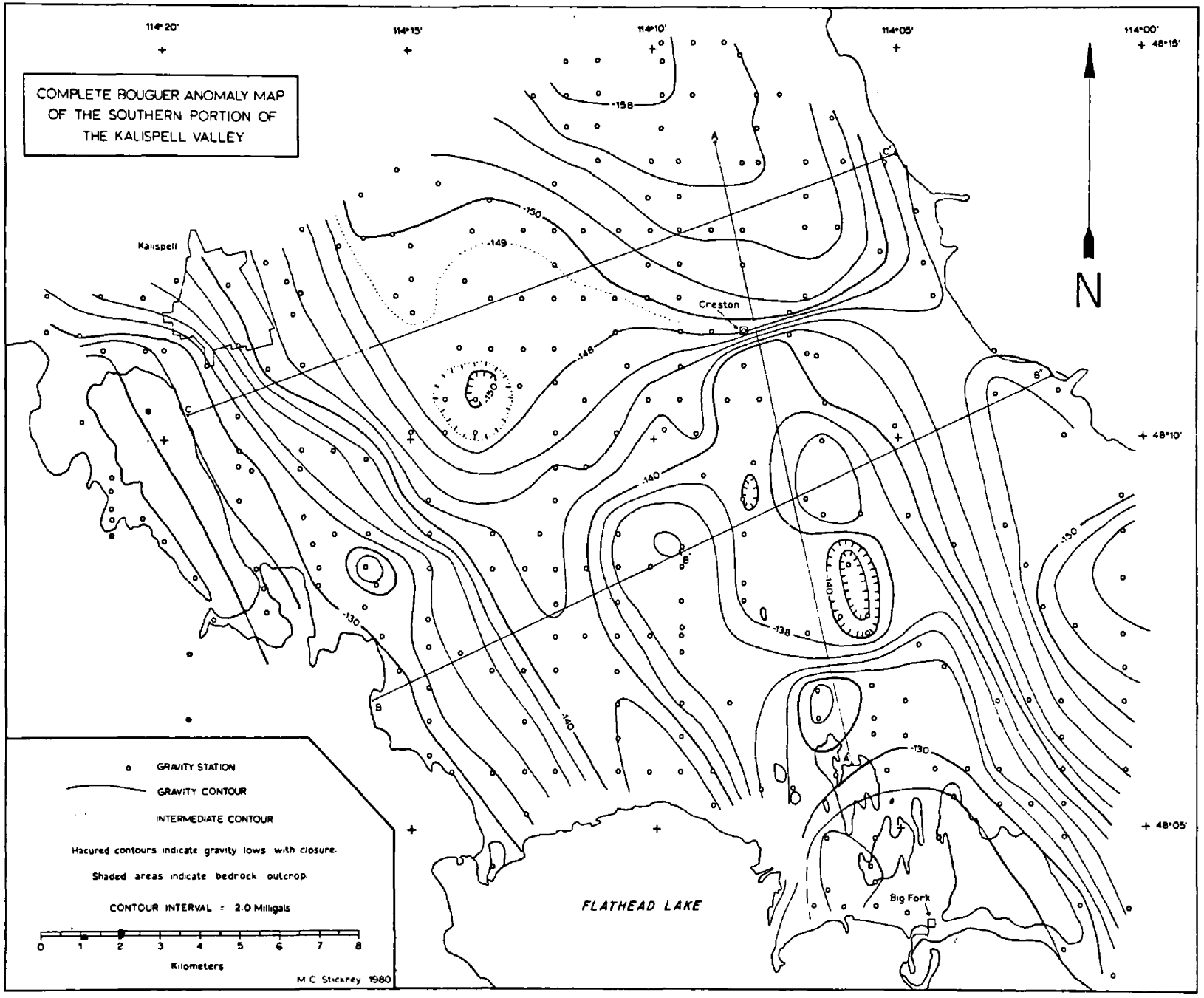
COMPLETE BOUGUER ANOMALY MAP
OF THE SOUTHERN PORTION OF
THE KALISPELL VALLEY
114°20'
114°15'
114°10'
114°05'
114°00'
48°15'
48°10'
48°05'
N
Kalispell
Creston
Big Fork
FLATHEAD LAKE
A
A'
B
B'
C
C'
-158
-150
-149
-148
-140
-138
-130
GRAVITY STATION
GRAVITY CONTOUR
INTERMEDIATE CONTOUR
Hacured contours indicate gravity lows with closure.
Shaded areas indicate bedrock outcrop
CONTOUR INTERVAL = 2.0 Milligals
0 1 2 3 4 5 6 7 8
Kilometers
M C Stickney 1980

Valley. Several small (two to four milligal) gravity highs and lows occur in the southern half of the map area. In the same way that -130 milligal contour surrounds most bedrock outcrop in the south and west parts of the map, the -140 milligal contour surrounds all but one of the minor gravity anomalies. This fact together with the small spatial extent of the anomalies suggest that the sources lie at relatively shallow depths. In general, a gravity survey cannot detect anomalies which have dimensions smaller than the distance between gravity stations. This gravity survey has an average station spacing of 1.3 kilometers, however, the station spacing is significantly greather than this in the central eastern part of the map area. The -146 milligal contour appears to bound the bedrock outcrop at the foot of the Swan Range along the northeast side of the Kalispell Valley.

The gravity in Figure 2 generally agrees with lower resolution, regional Bouguer gravity maps which cover the Kalispell Valley (Konizeski and others, 1968; and Bonini and others, 1973). However, the computed Bouguer anomalies in Figure 2 are consistently 9.6 milligals greater than those shown on the earlier maps. This difference stems from the formulas used to compute theoretical, sea level values of gravity. Bonini and others (1973) and Konizeski and others (1968) used the International Gravity Formula of 1930 (see Dobrin, 1960, page 234). I used the updated Gravity Formula 1967 given by the Defense Mapping Agency which has the form:

$$G = 978031.85\ (1 + 0.005278795\ \sin^2 LAT + 0.000023462\ \sin^4 LAT)$$

where G is theoretical gravity in milligals and LAT is latitude of the gravity station in degrees.

Interpretation and Discussion of the Gravity Data

Regional mapping by Johns (1970) shows that sedimentary rocks of the Precambrian Belt Supergroup crop out on all sides of the Kalispell Valley. Belt rocks are probably also present under the Cenozoic deposits in the Kalispell Valley. The observed gravity lows must result from the variable thickness of the low density Cenozoic deposits. A value of 2.2 grams per cubic centimeter was assumed for the Cenozoic deposits, the same value given in the HANDBOOK OF PHYSICAL CONSTANTS (1942) for water saturated sedimentary material of Tertiary or Quaternary age. The actual density may vary as much as 10% from this value depending on the degree of sorting, porosity, compaction, cementation and composition of the sediments. Several workers have measured the densities of rocks along the Rocky Mountain Trench in southern British Columbia. Thompson (1962) determined an average density of 2.69 $\pm$ 0.12 grams per cubic centimeter from 35 samples of Precambrian quartzite, limestone and argillite from the Cranbrook, British Columbia area. Spence and others (1972) determined a similar density of 2.70 + 0.12 grams per cubic centimeter from 42 samples of Precambrian sedimentary rocks collected near Radium, British Columbia. It seems reasonable to assume that similar Precambrian sedimentary rocks around the Kalispell Valley would have similar densities of approximately 2.7 grams per cubic centimeter. These densities indicate that the Cenozoic

deposits filling the Kalispell Valley have a density 0.5 grams per cubic centimeter less than the surrounding Belt rocks.

Before modeling the observed gravity anomalies, one must decide whether the regional gravity changes over the area and whether these changes result from the structures of interest. One attempt to estimate the regional gravity changes consists of fitting the best first, second, third and fourth order polynomial surfaces to the observed Bouguer gravity values. Each successively higher order polynomial surface gives a better fit to the observed data. However, these computed surfaces do not accurately reflect the regional gravity around the valley. Over 95% of the gravity measurements are within the Kalispell Valley while the remaining measurements were taken close to the edge of the valley. The gravity effect of the Kalispell Valley should extend several kilometers beyond the valley's edge. Therefore, the polynomial surfaces computed from gravity readings within the valley are biased by the large number of low gravity values associated with the valley. An alternate method for determining the regional gravity changes involves estimation from a map which covers the entire region such as the Complete Bouguer Anomaly Map of Montana (Bonini and others, 1973). A section of this map, reproduced in Figure 3, shows that the gravity contours roughly parallel the Rocky Mountain Trench. Note the large gravity low in the northeastern corner of the Kalispell Valley whose extension into the study area strongly affects the computed polynomial surfaces. Bouguer anomaly values of -130 to -140

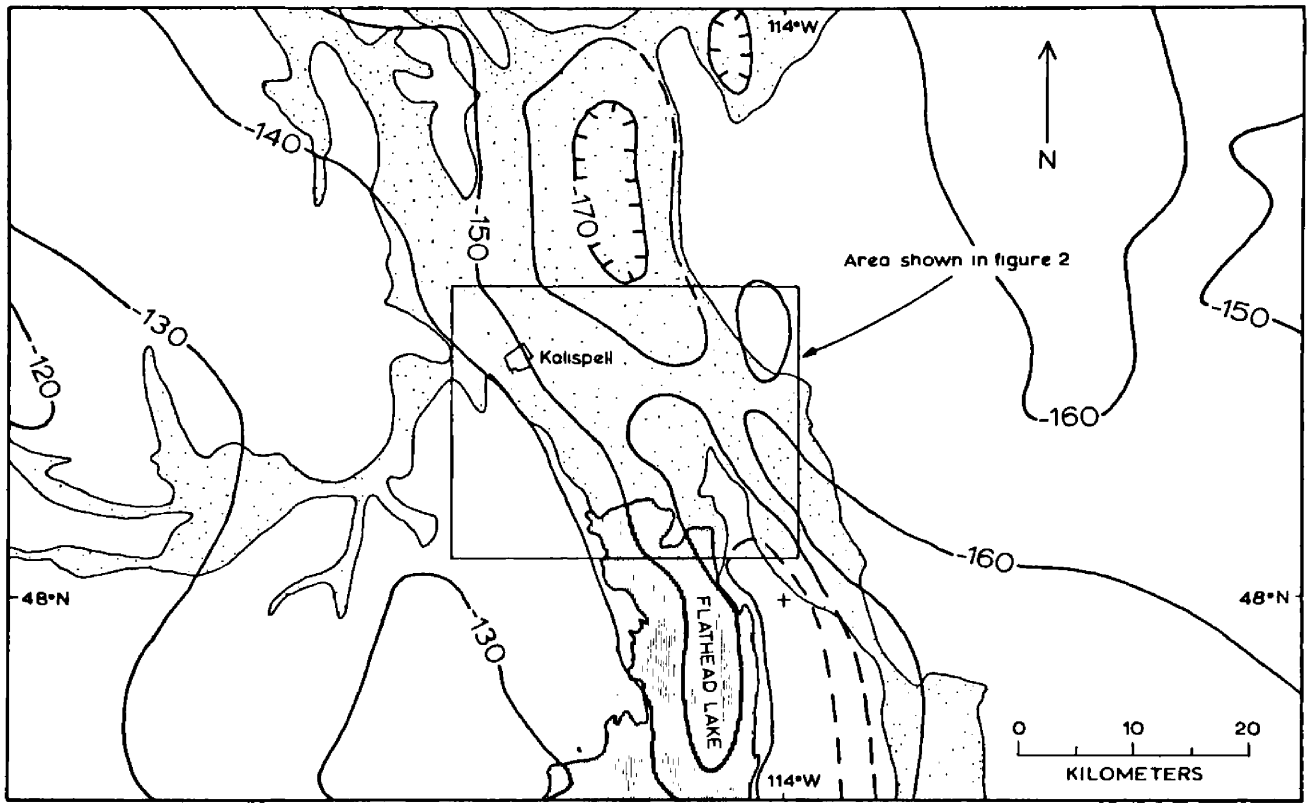

Figure 3. A portion of the COMPLETE BOUGUER ANOMALY MAP OF MONTANA (Bonini and others, 1973). Stippled area shows the distribution of Quaternary deposits.

milligals exist west of the Kalispell Valley while values of -150 to -160 milligals exist east of the valley. This 10 to 20 milligal decrease from the southwest side to the northeast side of the valley along a line striking N60E represents a regional change in gravity unrelated to the low density Cenozoic deposits filling the Kalispell Valley.

Cross section A-A' (Fig. 2) strikes N13W, at approximately 70 degrees to the direction of maximum regional change; a regional gravity profile of 0.22 milligals per kilometer was subtracted from the gravity profile along A-A' shown in Figure 4. The two large step-shaped anomalies in profile A-A' are modeled as bedrock offset along vertical faults, the north side downthrown relative to the south side. Telford and others (1976) give equations for the gravity effect of a semi-infinite, thick, horizontal slab, which when applied to cross section A-A' suggest the following bedrock configurations. The southern step in A-A' represents about 360 meters of offset in the bedrock surface. There are too few gravity stations to constrain precisely the slope or the gradient of this anomaly. However, bedrock on the upthrown side must lie near the surface since it outcrops about one kilometer south of the anomaly on profile A-A'. The northern step-shaped anomaly represents at least 570 meters of offset in the bedrock surface and is here called the Creston fault since it passes directly under the town of Creston. The slope of the anomaly suggests that the top of the step lies about 50 meters below the valley surface. The cumulative

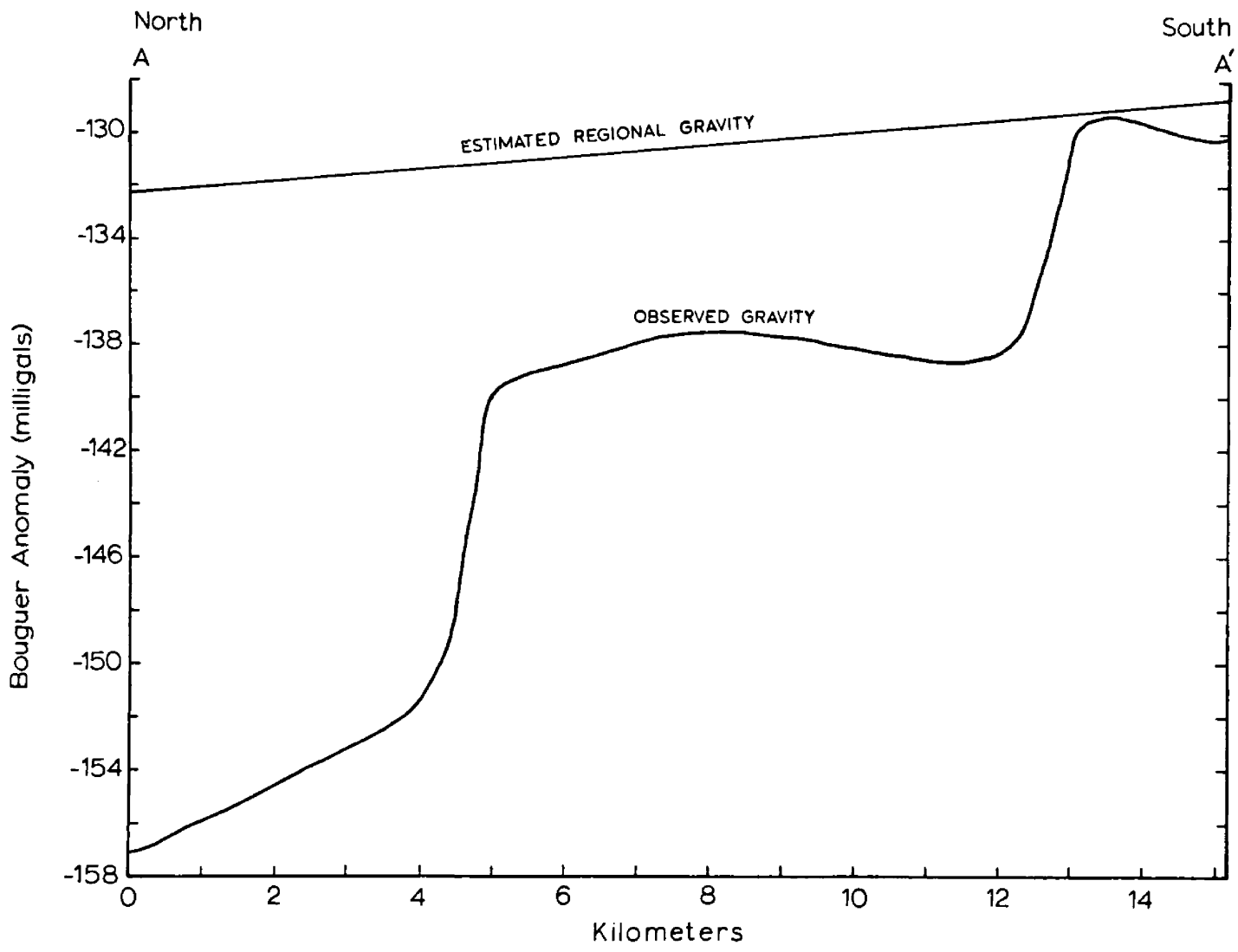

Figure 4. Observed Bouguer gravity and estimated regional gravity along profile A-A'.

offset of the two steps suggest a thickness of 900+ meters of low density sediments near A. One problem exists, however; the depth to bedrock calculated at the base of the southern step is about 300 meters below the depth to bedrock calculated at the top of the Creston fault, even though both places have the same Bouguer gravity value. In the semi-infinite, thick, horizontal slab equations, the thickness of the slab (the offset along a vertical fault) is calculated from the equation:

$$t = \Delta g/0.0128\rho$$

where t is the slab thickness in feet, Δg is the amplitude of the anomaly in milligals, and ρ is the density contrast between valley fill and bedrock in grams per cubic centimeter. The depth to the top of the slab is calculated from the equation:

$$d = t/e^{(245.7\ \rho\ dg/dx)_{-1}}$$

where d is the depth to the top of the slab, t is slab thickness in feet, ρ is the density contrast, and dg/dx is the maximum rate of change of gravity with horizontal distance (maximum gradient) in milligals per foot. The calculated depth depends mainly on dg/dx, the gradient. As Figure 2 shows, gravity stations to the north and south of the Creston fault anomaly constrain its position and amplitude, but no stations exist within the anomaly to constrain the gradient. A change of 3.3×10^{-3} milligals per meter in the observed gravity gradient will change the depth to bedrock calculated by about 75 meters. Additional gravity measurements taken within the gradient

would help to determine whether it is as steep as shown by the present contours. Another possible explanation for the steeper than expected gradient might be an underestimated regional gravity gradient which has a component dipping to the north. Removing a greater north-dipping, regional gravity gradient would result in a more moderate anomaly gradient than presently observed and hence, a greater calculated depth to the top of the slab. The discrepancy might also result from improperly assuming that offset along the Creston fault resembles a semi-infinite, horizontal slab.

Cross section B-B'' strikes N65E across the Kalispell Valley. The linear, trough-shaped anomaly which strikes northwest between B and B' suggests a graben, a down-dropped block bounded on each side by parallel normal faults. An anomaly whose length is several times its depth can be modeled as a two-dimensional structure using the technique of Talwani and others (1959). Before modeling the graben, the northeast-dipping regional gravity profile estimated from the state gravity map was subtracted. Figure 5 shows the Bouguer gravity profile and the regional profile estimated along cross section B-B''. Figure 6 shows the observed gravity profile after subtracting the regional gravity profile and the calculated bedrock profile between B and B'. Cross section B'-B'' was not modeled owing to the paucity of data in this part of the map area. The most steeply dipping bedrock surfaces shown in Figure 6, flank the deepest part of the valley and probably represent normal faults dipping into the graben. The linear

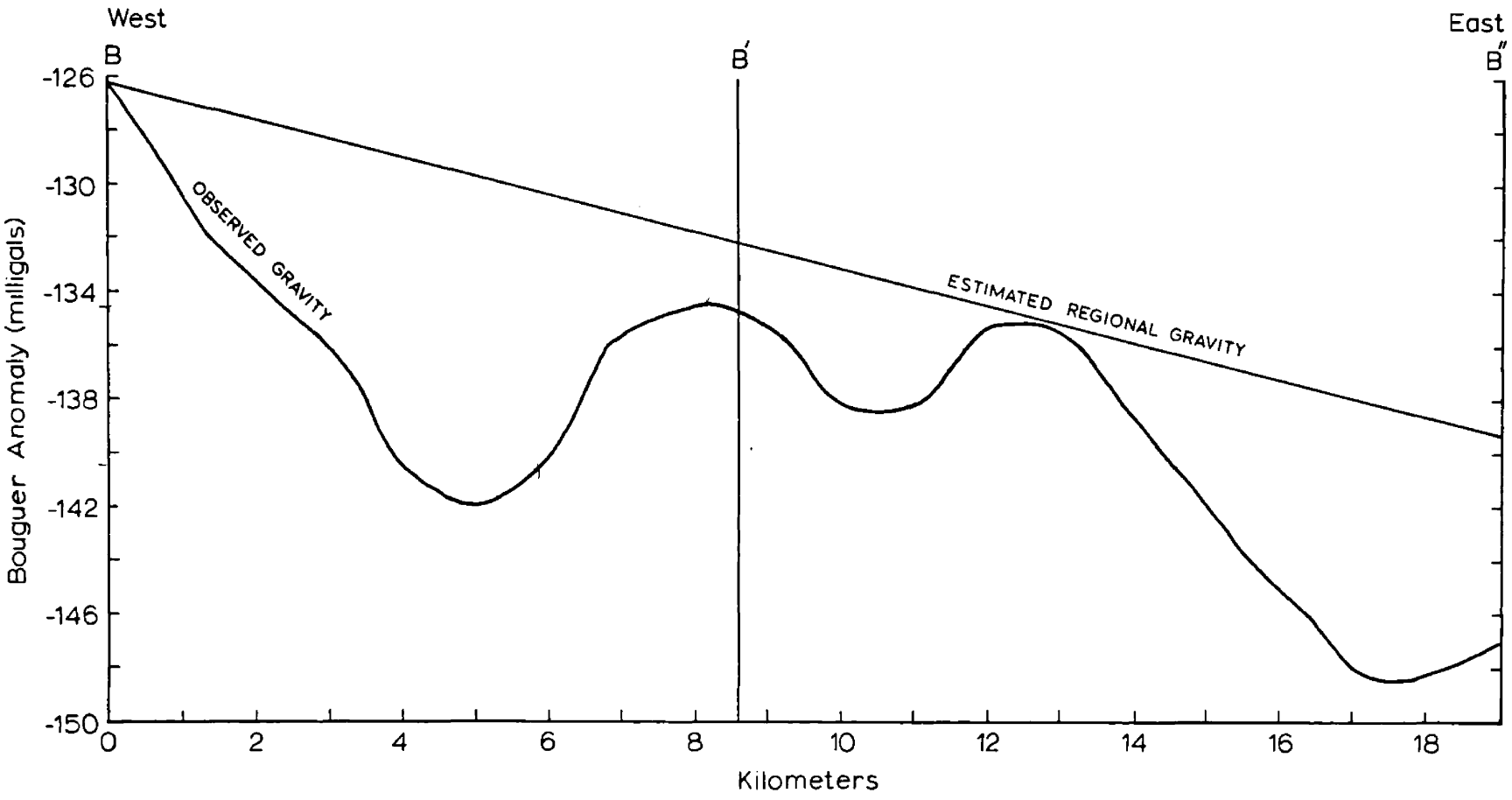

Figure 5. Observed Bouguer gravity and estimated regional gravity along profile B-B''.

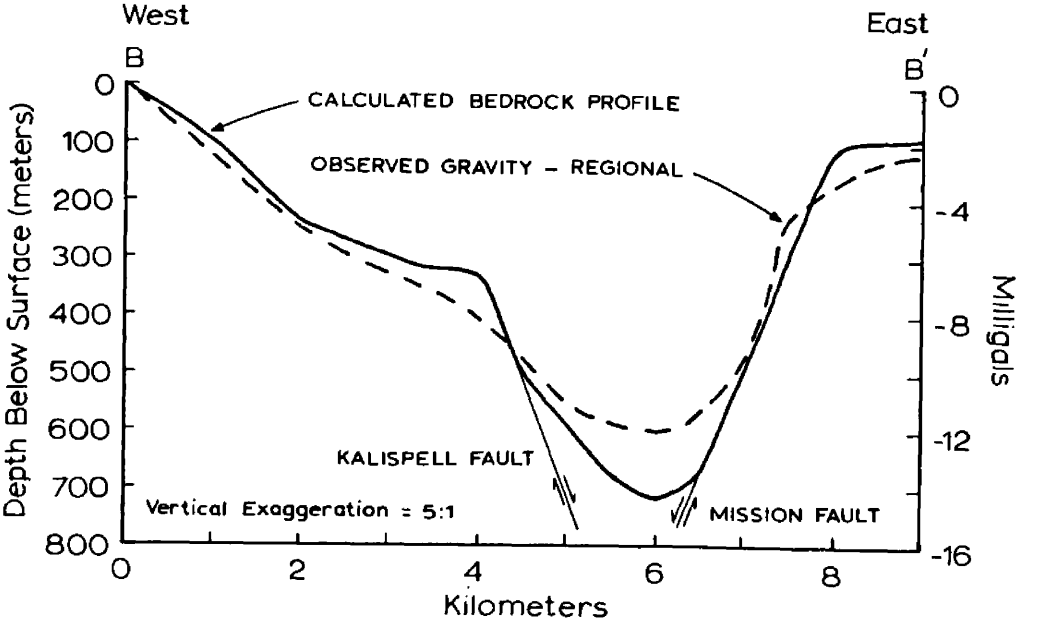

Figure 6. Adjusted gravity profile and calculated bedrock profile showing inferred faults along profile B-B'.

gravity gradient (Fig. 2) which strikes southeast from Kalispell to the north end of Flathead Lake, here called the Kalispell fault, is interpreted as the expression of the fault bounding the southwestern edge of the Kalispell Valley. It forms the southwest edge of the graben in the southern half of the map area. The parallel fault which strikes northwest from the Flathead River delta is probably the northern end of the Mission Fault. Bedrock offset along the Mission Fault appears to end near the center of the map where it meets the Creston fault. Modeling results suggest that the central part of the graben, which I call the Flathead graben, contains roughly 700 meters of low density material. The central third of cross section B-B'' shows highs and lows possibly associated with buried bedrock topography along the northern extension of the Mission Range. Gravity reaches its lowest value along the northeastern third of this cross section where the Swan Valley joins the Kalispell Valley. The linear gravity anomaly which parallels the eastern edge of the Mission Range suggests the presence of a steep fault which drops the floor of the Swan Valley down to the east and brings the Mission Range up to the west.

Cross section C-C' traverses the Kalispell Valley about eight kilometers north of, and parallel to, cross section B-B'. Cross section C-C' lies north of the Creston fault which terminates the gravity high associated with the northern end of the Mission Range. Figure 7 shows the observed Bouguer anomaly along C-C' and the northeast-dipping regional gravity profile estimated from the state gravity

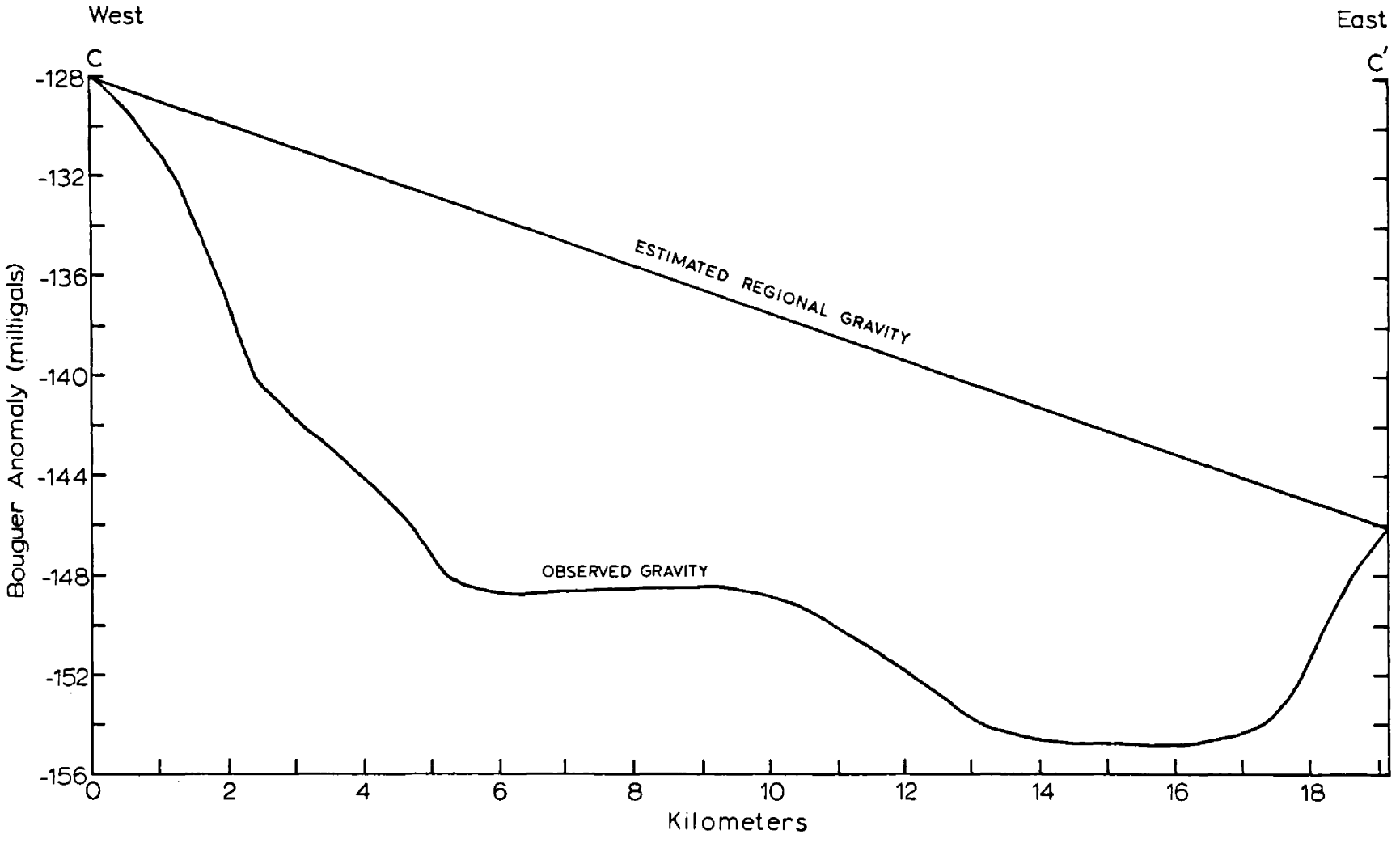

Figure 7. Observed Bouguer gravity and estimated regional gravity along profile C-C'.

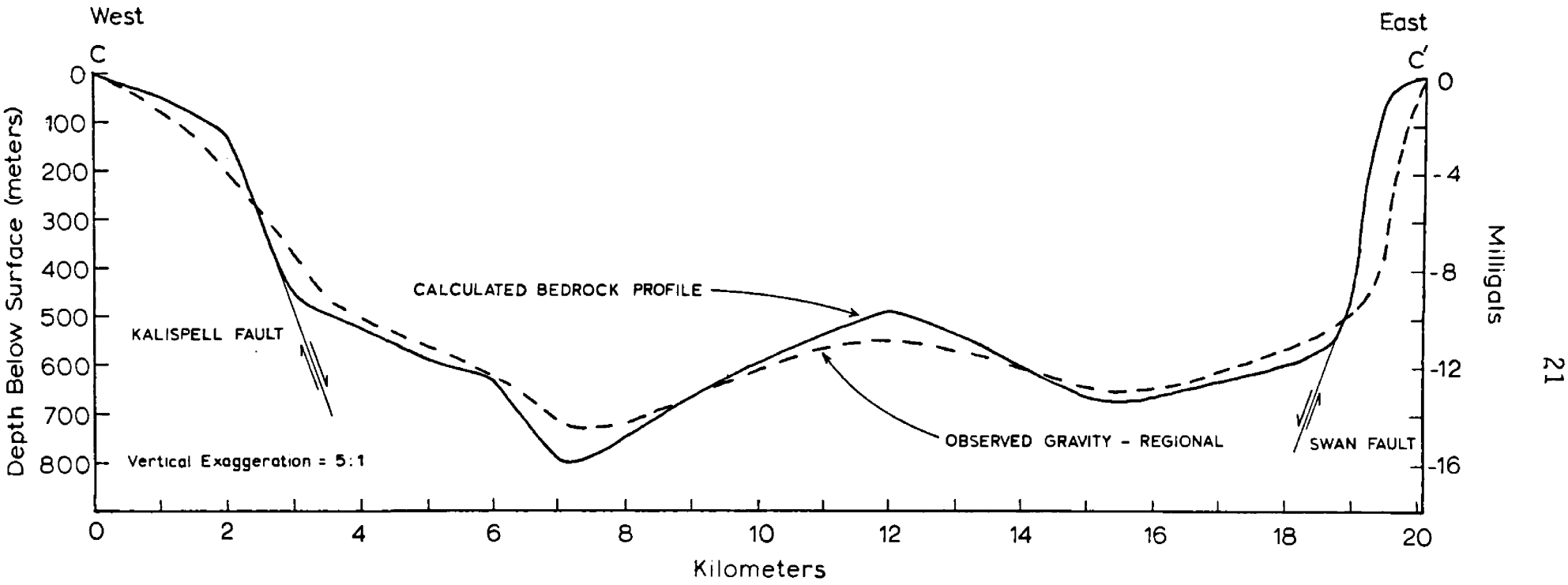

Figure 8. Adjusted gravity profile and calculated bedrock profile showing inferred faults along profile C-C'.

map. Figure 8 shows the gravity profile after subtracting the regional gravity profile and the calculated bedrock profile. The calculated bedrock surfaces dip steeply near the edges of the valley, revealing the valley-bounding faults. The Swan Fault along the eastern edge of the valley has about 500 meters of relief below the valley fill. The Kalispell fault runs along the western valley edge and has roughly 400 meters of relief. A maximum depth of 800 meters of valley fill occurs one third of the way between C and C'. The bedrock floor of the Kalispell Valley lies at an average depth of 550 meters below the surface and has up to 300 meters of relief.

CHAPTER III

KALISPELL VALLEY SEISMICITY

University of Montana Earthquake Data and Results

Although the National Oceanic and Atmospheric Administration (NOAA) World Earthquake Data File Summary contains only four epicenters near the Kalispell Valley north of 48 degrees latitude before 1975, recent earthquakes demonstrate continued movement along some faults in the Kalispell Valley. A search of United States Earthquakes (annual publication, 1928-1968) yields numerous reports of felt earthquakes of local origin dating back to 1935. At least 25 earthquakes have shaken the Kalispell-Bigfork area since 1935 without noticeably affecting the surrounding region. The lack of sufficient instruments capable of detecting earthquakes less than about magnitude 4 makes instrumental epicenter locations of smaller quakes uncertain and incomplete before 1974. During 1974, the Geology Department at the University of Montana installed eight seismograph stations between Helena and Missoula, bringing the number of seismograph stations operated by the University to 17. An array of four stations around Lake Koocanusa (Libby array), four stations around the Dworshak Reservoir in Idaho (Orofino array), eight stations between Missoula and Helena (Helena array), the World Wide Standardized Seismograph Network (WWSSN) Station near Missoula (MSO) and the U.S.G.S. station near Hungry Horse Dam

(HHM) all recorded earthquakes which began to occur in the Kalispell Valley late in 1974 and continued to occur through the closure of the University of Montana arrays in October, 1976.

I used arrival times of P- and S-waves recorded at surrounding seismograph stations and the computer program HYPOELLIPSE (Lahr, 1979) to determine hypocentral parameters for 98 Kalispell Valley earthquakes which occurred between August, 1974 and October, 1976 and ranged in magnitude from about 1.5 to 5.0. In order to locate the earthquakes, a seismic velocity model of the layers which comprise the crust and upper mantle of the earth must be specified. Several workers (Meyer and others, 1961; McCamy and Meyer, 1964; Asada and Aldrich, 1966; Bennett and others, 1975; and Walton and others, 1972) have recorded explosions in northwestern Montana and southern British Columbia and have calculated models of crustal structure from their data. Six different crustal models from their studies were tested using HYPOELLIPSE to locate 21 of the largest and best recorded Kalispell Valley earthquakes. The standard errors of the origin time, focal depths, root mean square of the travel time residuals and the estimated horizontal and vertical errors of the hypocenters were compared for each of the 21 earthquakes when located by each of the six crustal models. Table 1 lists the P-wave velocities of the crustal model determined by Walton and others (1972) which gave consistently better results than the other crustal models and was used to locate all earthquakes shown in Figures 11 and 14 and listed in Appendix 3.

S-wave velocities are determined by dividing the P-wave velocities by 1.76.

Table 1

Crustal and upper mantle P-wave velocity used to locate the Kalispell Valley earthquakes

Velocity km/sec	Depth to Layer Top km
5.90	0
6.50	25
7.95	43

The two-layer model of Walton and others (1972) is similar to the more complex model proposed by McCamy and Meyer (1964).

All Kalispell Valley earthquake magnitudes were determined from the WWSSN station MSO (except the February 4, 1975 earthquake which drove the short period instruments off scale) by measuring the period and amplitude of the largest pulse on each short period horizontal instrument (magnification = 100,000 at 1 Hz) and calculating the amount of true ground displacement. When this value is multiplied by 2800, one obtains the amplitude that would have been recorded by standard Wood-Anderson seismographs (magnification 2800). The magnitude is computed from the epicentral distance and the estimated Wood-Anderson amplitude using the relation developed by Richter (1958, page 340). Figure 9 shows the cumulative number of earthquakes in the Kalispell Valley plotted against their magnitudes. The alignment of

Figure 9. Graph of the number of Kalispell Valley earthquakes larger than a particular magnitude (the cumulative number) versus their magnitude. All magnitudes were determined from MSO except the magnitude 5.0 earthquake of February 4, 1975.

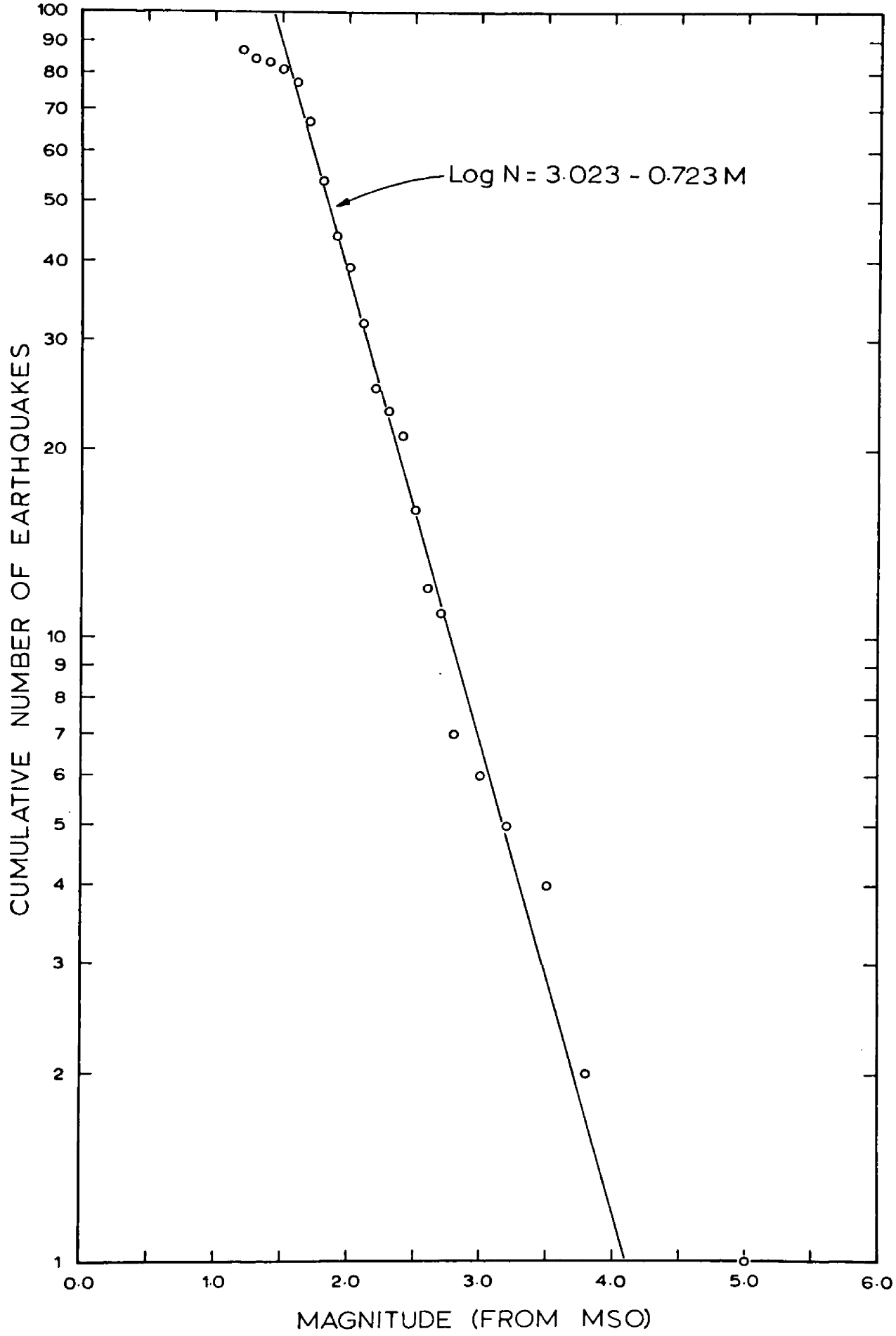
Log N = 3.023 - 0.723 M
CUMULATIVE NUMBER OF EARTHQUAKES
MAGNITUDE (FROM MSO)
100
90
80
70
60
50
40
30
20
10
9
8
7
6
5
4
3
2
1
0.0
1.0
2.0
3.0
4.0
5.0
6.0

data points between magnitudes 1.7 and 4.0 suggests that the University of Montana data are complete for earthquakes with magnitudes as small as 1.7. The equation:

$$\text{Log } N = 3.023 - 0.723M$$

satisfies the data with magnitudes between 1.7 and 4.0 where N is the cumulative number of earthquakes, and M is the magnitude calculated from station MSO. The constant 0.723, preceeding the magnitude term (the "b value") for these earthquakes falls near the lower end of the range of observed b values for Montana earthquakes (Qamar and Breuninger, 1979). Figure 10 shows the number of quakes per week in the Kalispell Valley and the estimated radiated seismic energy per week. Radiated energy was estimated from the magnitude of each earthquake by the relation:

$$\text{Log } E = 9.9 + 1.9\ M_L - 0.024\ M_L^2$$

where E is energy in ergs and M_L is the estimated Richter or "local" magnitude (see Richter, 1958, page 366). A peak in the seismic activity occurred during late January and early February, 1975; the largest earthquake ever recorded in the Kalispell Valley occurred during this period on February 4. Figure 10 shows that earthquakes occurred monthly from the peak of activity early in 1975 through June, 1976. From early February to mid-October, 1975, the radiated seismic energy decreases, similar to the decrease in seismic energy observed for aftershocks following a main shock. After October, 1975, scattered peaks of radiated seismic energy suggest swarm-type activity.

Figure 10. Number of earthquakes per week (solid bars) recorded by the University of Montana and the radiated seismic energy per week (open bars). Energy estimated from magnitude using the relation from Richter (1958, page 366).

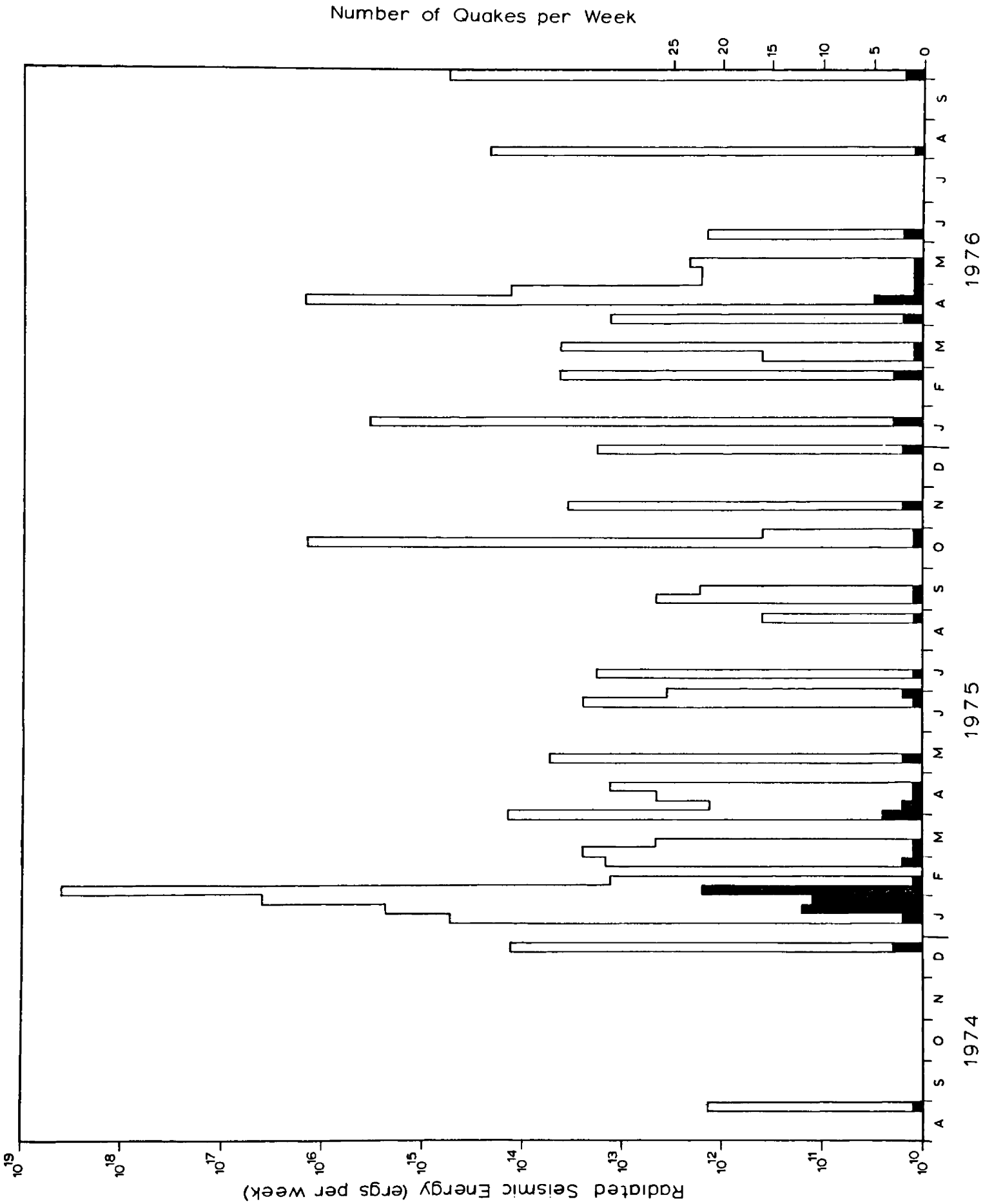
Number of Quakes per Week
25
20
15
10
5
0
A S O N D J F M A M J J A S O N D J F M A M J J A S O N D J F M A M J J A S
1974
1975
1976
Radiated Seismic Energy (ergs per week)
10^{19}
10^{18}
10^{17}
10^{16}
10^{15}
10^{14}
10^{13}
10^{12}
10^{11}
10^{10}

Figure 11 shows Kalispell Valley earthquakes recorded by the University of Montana. Solid dots indicate epicenters with uncertainties less than six kilometers; error bars are plotted for these quakes which have magnitudes of 2.0 or greater. About 85% of these earthquakes occur in a zone 6 kilometers wide and 20 kilometers long which trends northeast-southwest. The long axis of the zone lies about 5 kilometers south of, and roughly parallel to the Creston fault. A special feature of HYPOELLIPSE is its calculation of the standard error of hypocentral position in the directions of maximum and minimum uncertainty. Because most of the readings used to locate the Kalispell Valley earthquakes come from the Libby array to the northwest and the Helena array to the southeast, the direction of maximum epicentral uncertainty is in the northeast-southwest direction. Most earthquakes have estimated errors two to three times greater in the northeast-southwest direction than in the northwest-southeast direction. Unfortunately, the direction of maximum uncertainty corresponds to the trend of the zone of epicenters. In addition, two of the larger earthquakes (magnitudes 5.0 and 3.5) located without P- and S-wave readings from HHM fall on the southwest end of the zone. Preliminary epicenters of other earthquakes lacking HHM readings fall near the northwest corner of Flathead Lake, but when readings from HHM were added to their solutions, they shifted to the northeast. This fact suggests that the two larger earthquakes located west of the Flathead River probably occurred east of the Flathead River. Therefore, the apparent

Figure 11. Epicenter map of Kalispell Valley earthquakes recorded by the University of Montana Earthquake Research Lab between August, 1974 and October, 1976. Open circles indicate epicenters with uncertainties greater than six kilometers. Solid circles show epicenters with uncertainties less than six kilometers. Size of the solid circles are proportional to magnitude. Error bars indicate the amount and direction of the maximum and minimum epicentral uncertainty for the better located quakes with magnitudes of 2.0 or greater. See Table A2 for hypocenter parameters.

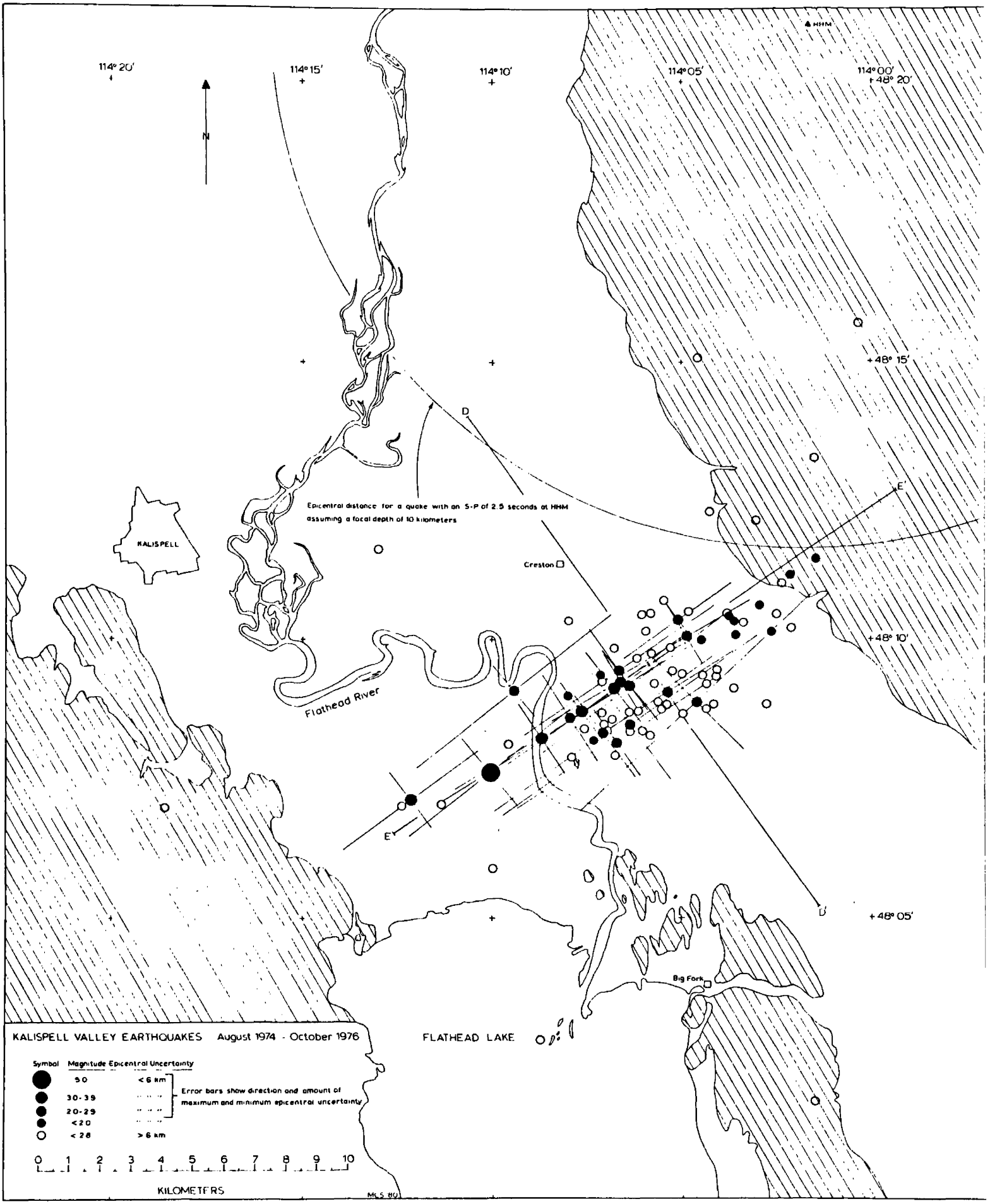
114° 20'
114° 15'
114° 10'
114° 05'
114° 00'
+48° 20'
+48° 15'
+48° 10'
+48° 05'
N
HHM
D
D'
E
E'
Epicentral distance for a quake with an S-P of 2.5 seconds at HHM assuming a focal depth of 10 kilometers
KALISPELL
Creston
Flathead River
Big Fork
FLATHEAD LAKE
KALISPELL VALLEY EARTHQUAKES August 1974 - October 1976
Symbol
Magnitude
Epicentral Uncertainty
5.0
3.0-3.9
2.0-2.9
<2.0
<2.8
<6 km
>6 km
Error bars show direction and amount of maximum and minimum epicentral uncertainty
0 1 2 3 4 5 6 7 8 9 10
KILOMETERS
MLS 80

zone of epicenters may not define a northeast trending fault but may result instead from systematic errors in the earthquake locations. However, other data suggest that the earthquakes may, in fact, have occurred on a northeast trending fault.

The predominant travel time difference between S- and P-waves (S-P time) of 2.5 seconds recorded at the nearby station HHM for the majority of these events supports the hypothesis that most of these earthquakes occurred at the same location within the resolution of the data. However, some of the earthquakes have S-P times at HHM ranging from 1.9 to 3.2 seconds. The 1.3 second variation in the observed S-P time might result from distribution of the earthquakes along the Creston fault. Variation of focal depths between 0 and 15 kilometers could produce an S-P variation of only 0.7 seconds. Two perpendicular cross sections (Fig. 12) plotted through the cluster of epicenters (D-D' and E-E' in Figure 11) illustrate the range of focal depths computed for these events and their distribution along the northeast-trending zone. Cross section D-D' shown in Figure 12a strikes across the Creston fault, E-E' (Fig. 12b) strikes along it. Figure 12a suggests that the hypocenters fall on a steeply dipping plane, and hypocentral error as indicated by the error bars, cannot explain all of the observed range in focal depth. Further evidence of faulting along a northeast-striking fault comes from P-wave first motion data. For each quake, HYPOELLIPSE plots the vertical direction of P-wave first motions where their ray paths pierce a lower-hemisphere, equal area

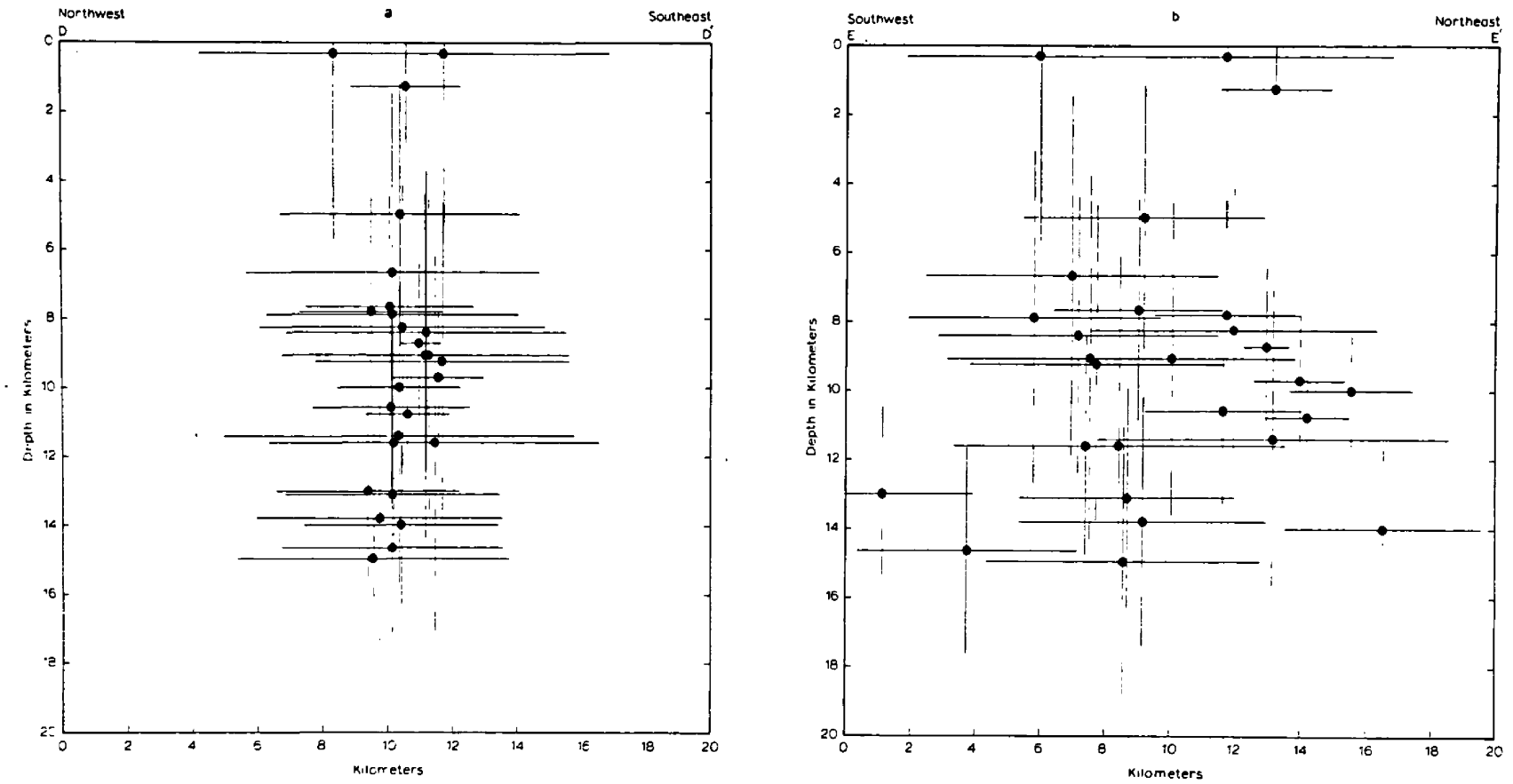

Figure 12. Orthogonal cross sections of the 28 Kalispell Valley earthquakes recorded by the University of Montana with epicentral uncertainties of six kilometers or less. Cross section D-D' strikes across the Creston fault, E-E' strikes along it. Error bars show the hypocentral uncertainties calculated by HYPOELLIPSE.

projection centered on the hypocenter. One graphically computes a fault plane solution by dividing opposite first motions into quadrants with two orthogonal great circles which represent perpendicular planes (the fault plane and the auxiliary plane). Although additional data is required to determine which great circle (nodal plane) represents the fault plane, a fault plane solution provides information such as the type of faulting and the approximate stress orientations required to produce faulting. The first motion pattern is sensitive to the crustal model used to locate the earthquakes. Though constant velocity crustal layers (Table 1) work well for epicenter location, a more realistic velocity model, in which velocity varies continuously with depth, produces more reasonable first motion plots. I used a crustal model in which the P-wave velocity increases at the rate of 0.06 kilometers per second per kilometer of depth. This rate of velocity increase with depth gives an upper mantle velocity similar to the upper mantle velocity determined by Walton and others (1972). When determining first motion patterns with this linear-velocity-increase-with-depth model, the hypocenters were held fixed at the coordinates determined from the layered crustal model of Walton and others (1972). The resulting fault plane solutions do not have artificial "rings" of first motions corresponding to the angle of incidence for mantle or mid-crustal head waves such as those observed with layered models.

Figure 13 shows fault plane solutions for the two largest Kalispell Valley earthquakes (Figs. 13a and 13b) and a composite fault

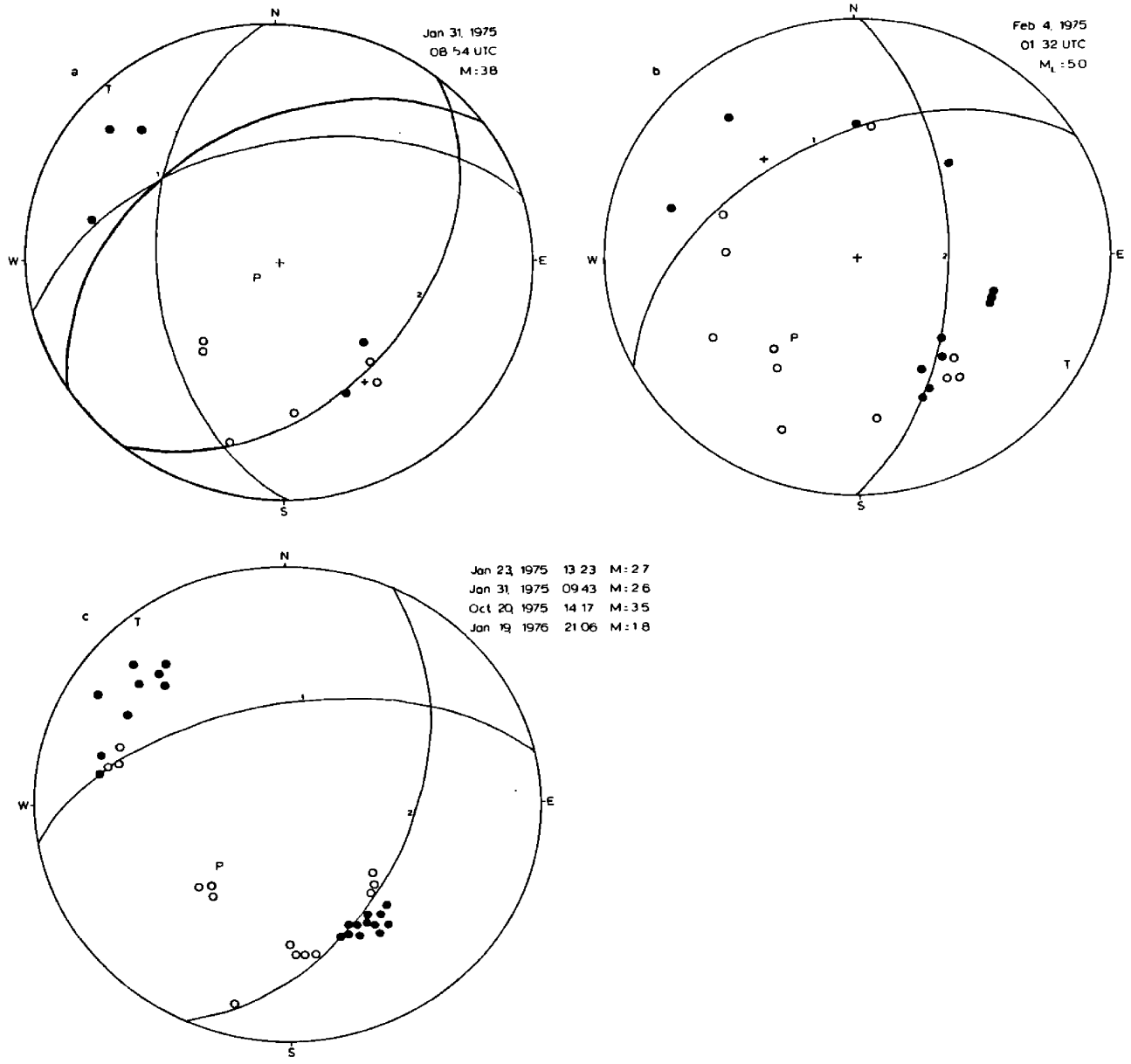

Figure 13. Lower hemisphere, equal area projections (fault plane solutions) showing compressional (solid circles), dilatational (open circles), weak compressional (+) and weak dilatational (-) P-wave first motions for six Kalispell Valley earthquakes. Theoretical axes of maximum and minimum compressive stress indicated by P and T respectively. Orientation of nodal planes and P-, T-axes are listed in Table 2. The shaded area in 13a shows the range of uncertainty for nodal plane 1. Figure 13c is a composite of first motions from four earthquakes.

Table 2. Orientations of Nodal Planes and P-, T-axes for the Fault Plane Solutions Shown in Figures 13 and 15.

Figure	Nodal Plane 1* strike	dip	Nodal Plane 2 strike	dip	P axis strike	plunge	T axis strike	plunge	Remarks
13 a	N55E	44NW	N40E	43SE	S60W	80SW	N45W	0 Hor.	Nodal plane 1 poorly constrained
13 b	N60E	50NW	N	60E	S38W	56SW	S60E	6SE	Largest Kalispell Valley quake
13 c	N80E	56NW	N24E	50SE	S48W	58SW	N38W	4NW	Composite of 4 quakes
15 a	N39E	58NW	N72W	62SW	S17E	3SE	N72E	46NE	Composite of 7 microearthquakes
15 b	N 3 W	57SW	N36E	40SE	N38E	69NE	N76W	10NW	Composite of 2 microearthquakes
15 c	N61E	44NW	N60W	64SW	N75E	54NE	S 3 W	12SW	

*Nodal plane 1 represents the preferred fault plane.

plane solution for four smaller but well recorded Kalispell Valley earthquakes (Fig. 13c). All three fault plane solutions suggest normal movement with subordinate amounts of strike-slip movement on a fault which strikes north to northeast. Figure 13b shows the first motion pattern for the magnitude 5.0 Kalispell Valley earthquake of February 4, 1975; first motion data from 13 additional stations within a distance of 1700 kilometers are also plotted.

Kalispell Valley Microearthquake Surveys and Results

To obtain more detailed information about hypocenters in the Kalispell Valley, A.I. Qamar and I operated five portable seismograph stations in the valley from the 19th to the 23rd of August, 1976. Again in 1979 from August 13 to September 10, I operated six seismograph stations in the Kalispell Valley to collect earthquake data at epicentral distances of 20 kilometers or less. Each seismograph station except BFM consisted of a Mark Products model L-4 short period vertical seismometer and a Sprengnether model MEQ-800 drum recorder. The data were recorded on smoked paper records at a rate of 60 millimeters per minute. Several minutes of the Bureau of Standards radio station WWV were recorded at the beginning and end of each record in order to measure the time correction and amount of internal clock drift. Clock drift never exceeded 0.15 seconds per day at any station. One can determine the time correction to the nearest 0.05 seconds using a 7 power magnifier with a scale graduated at 0.1 millimeter

intervals. The Earthquake Research Lab installed seismograph station BFM near Bigfork, Montana during March of 1979; it continues to operate through the present. FM radios telemeter the data from BFM to the University of Montana campus where an ink pen records the data on a drum recorder at a rate of 60 millimeters per minute.

The measured P- and S-wave arrival times of the Kalispell Valley earthquakes recorded during the field survey and HYPOELLIPSE were used to compute hypocenters. Figure 14 shows the locations of 14 earthquakes (listed in Table A3) which occurred in the Kalispell Valley during five weeks of recording with the portable networks. The magnitudes for all the earthquakes were estimated from the vertical ground motion using the "equivalent Wood-Anderson" method previously described. These calculated magnitudes are not true local magnitudes. While Richter used horizontal seismographs to define the local magnitude scale, I measured vertical ground motion. Also, the frequency responses differ between the University of Montana portable seismographs and the Wood-Anderson seismographs which Richter used. In spite of these differences, the relative magnitudes between the Kalispell Valley microearthquakes should be roughly correct. Earthquakes recorded during the surveys had magnitudes ranging between -1.5 and 0.

Generally, earthquakes occurring within the temporary network have estimated epicentral uncertainties less than two kilometers. Those events which occurred within 10 kilometers of, but outside the

Figure 14. Epicenter map of the Kalispell Valley microearthquakes recorded during the periods August 19 to 23, 1976 and August 13 to September 10, 1979. Dots show epicenters, bars indicate the amount and direction of maximum and minimum epicentral uncertainty. See Table A3 for hypocenter parameters. Solid triangles indicate seismograph stations, dates indicate the period of operation for temporary stations. Shading shows bedrock outcrop.

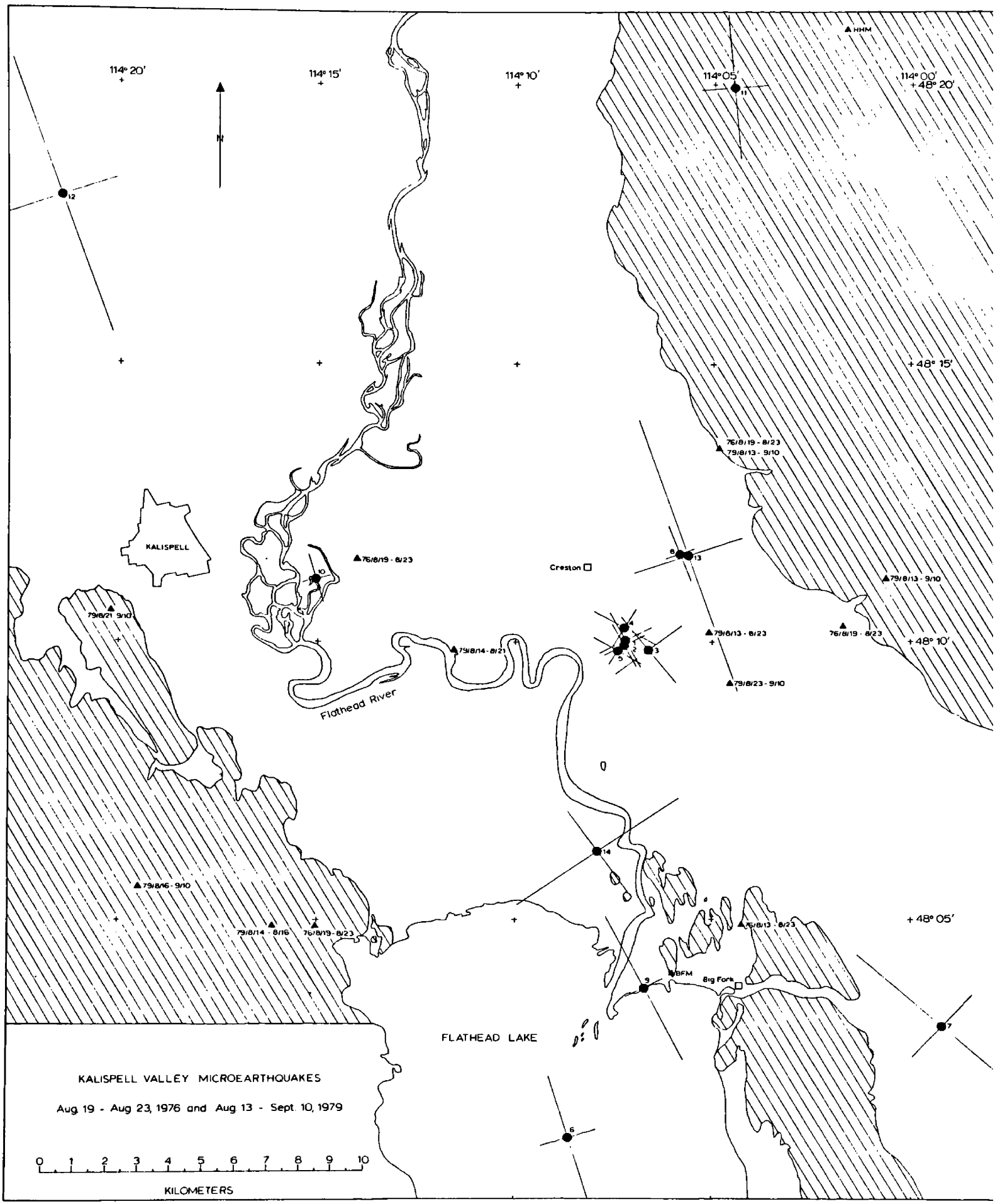
114° 20'
114° 15'
114° 10'
114° 05'
114° 00'
+48° 20'
+48° 15'
+48° 10'
+48° 05'
N
HHM
KALISPELL
Creston
Flathead River
FLATHEAD LAKE
Big Fork
BFM
76/8/19 - 8/23
79/8/13 - 9/10
79/8/14 - 8/21
79/8/21 - 9/10
79/8/16 - 9/10
79/8/14 - 8/16
KALISPELL VALLEY MICROEARTHQUAKES
Aug. 19 - Aug. 23, 1976 and Aug. 13 - Sept. 10, 1979
0 1 2 3 4 5 6 7 8 9 10
KILOMETERS

seismograph network, have epicentral uncertainties two to three times greater than those inside the network. Nine of the fourteen microearthquakes have well determined focal depths, which range from 7.5 to 13.6 kilometers below the surface with an average of 10 kilometers. The earthquakes numbered 1 through 5 in Figure 14 occurred on August 19, 1976 in a tight cluster just south of the Creston fault. All five events occurred within a 14 hour period; no other earthquakes were recorded for the following week. Earthquakes on August 20 and September 2, 1979 (numbered 8 and 13) occurred four kilometers northwest of the August 19, 1976 cluster. Figure 16a shows the first motions of these seven earthquakes plotted on an equal-area, lower hemisphere projection. The first motions constrain the two nodal planes well. The fault plane solution indicates a combination of reverse and strike-slip motion, an unexpected result in view of the nearby normal faults. The largest of the seven earthquakes had a magnitude of -0.1. Several other earthquakes occurred near the north end of Flathead Lake. At least two of these events probably occurred along the northern end of the Mission Fault. A composite fault plane solution for these events (numbered 9 and 14) suggests a north trending normal fault which dips west (Fig. 15b), in good agreement with the fault suggested by the gravity data. One microearthquake occurred five kilometers east of Kalispell near the intersection of the Kalispell and Creston faults (number 10). A fault plane solution for this event (Fig. 15c) suggests movement along an east-west normal fault, such as one might expect to

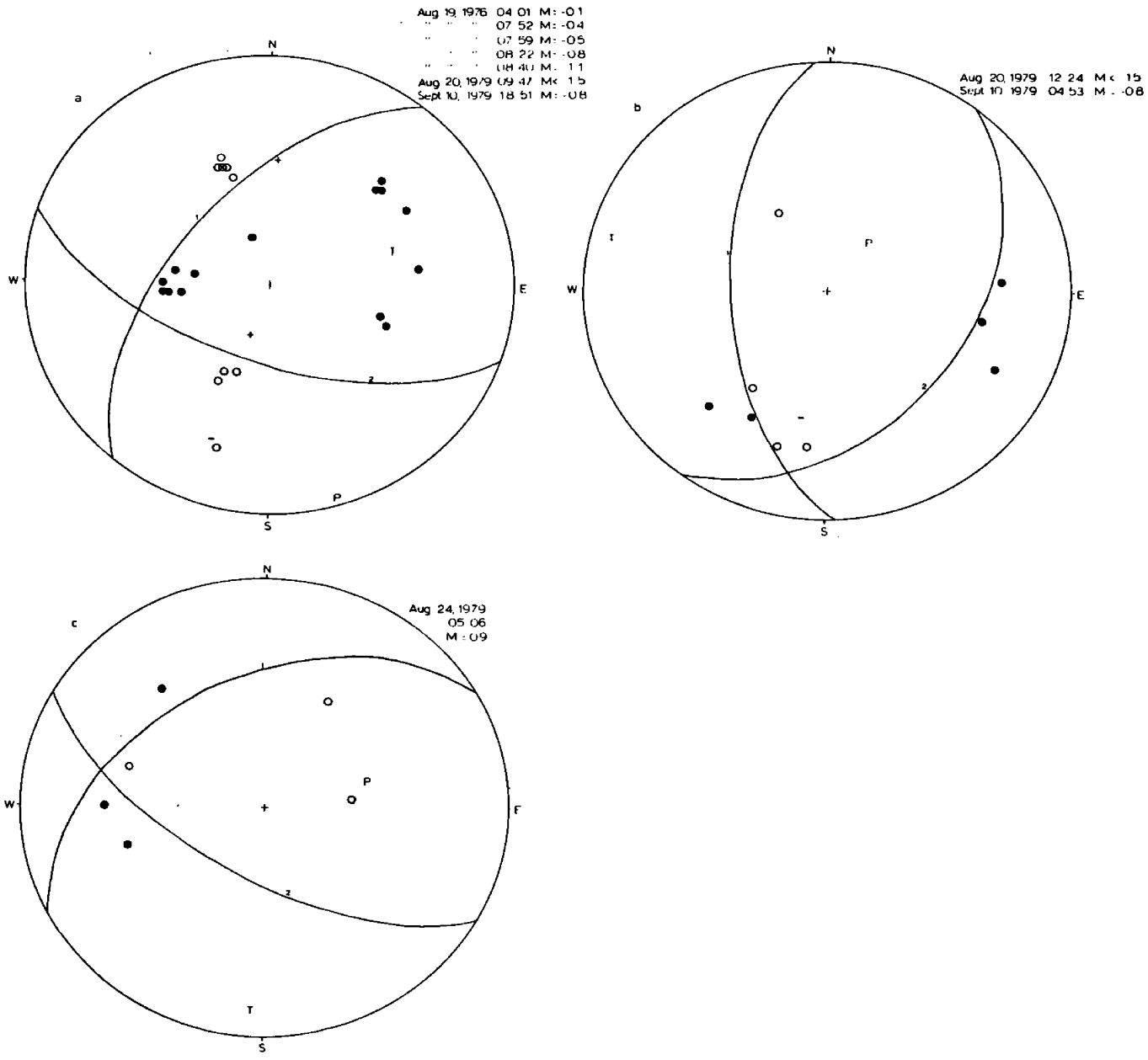

Figure 15. Fault plane solutions for 10 microearthquakes recorded in the Kalispell Valley. Figure 15a shows the first motions from seven events clustered near Creston (see Fig. 14); 15b shows the first motions from two events (numbered 9 and 14 in Fig. 14) near the north end of Flathead Lake; and 15c is from one microearthquake (number 10, Fig. 14) located five kilometers southeast of Kalispell. See Figure 13 of an explanation of of symbols.

find along the Creston fault. Two other earthquakes occurred north of the Creston fault, one near each side of the Kalispell Valley. First motion data were too sparse to determine a fault plane solution for these quakes, however, one might expect these earthquakes to result from normal slip along the Swan and Kalispell faults.

CHAPTER IV

DISCUSSION

Figure 16 shows the geology of the Kalispell Valley area from Johns (1970) and the faults inferred from gravity data. The Bouguer gravity map (Fig. 2) clearly indicates a fault (the Creston fault) trending northeast across the Kalispell Valley. Another fault, inferred from the gravity, occurs eight kilometers southeast of the Creston fault and agrees very well with one which Johns (1970) inferred from geologic mapping. Microearthquakes located within three kilometers of the Creston fault by nearby seismograph stations suggest that it is presently active. Although the earthquakes recorded by the University of Montana are located in an elongate zone, parallel to, and four to six kilometers southeast of, the Creston fault, I believe that these earthquakes, as a group, are mislocated somewhat to the south and actually originated along the Creston fault. As evidence, over 55% of these earthquakes have S-P intervals of 2.5 or 2.6 seconds at the nearest station, HHM. The arc drawn in Figure 11 shows the epicentral distance from HHM for a quake with an S-P of 2.5 seconds and a focal depth of 10 kilometers (the average focal depth of the quakes shown in Figure 11). The arc just touches the northeastern end of the zone of epicenters. Shifting all of the computed epicenters about five kilometers to the northwest would satisfy

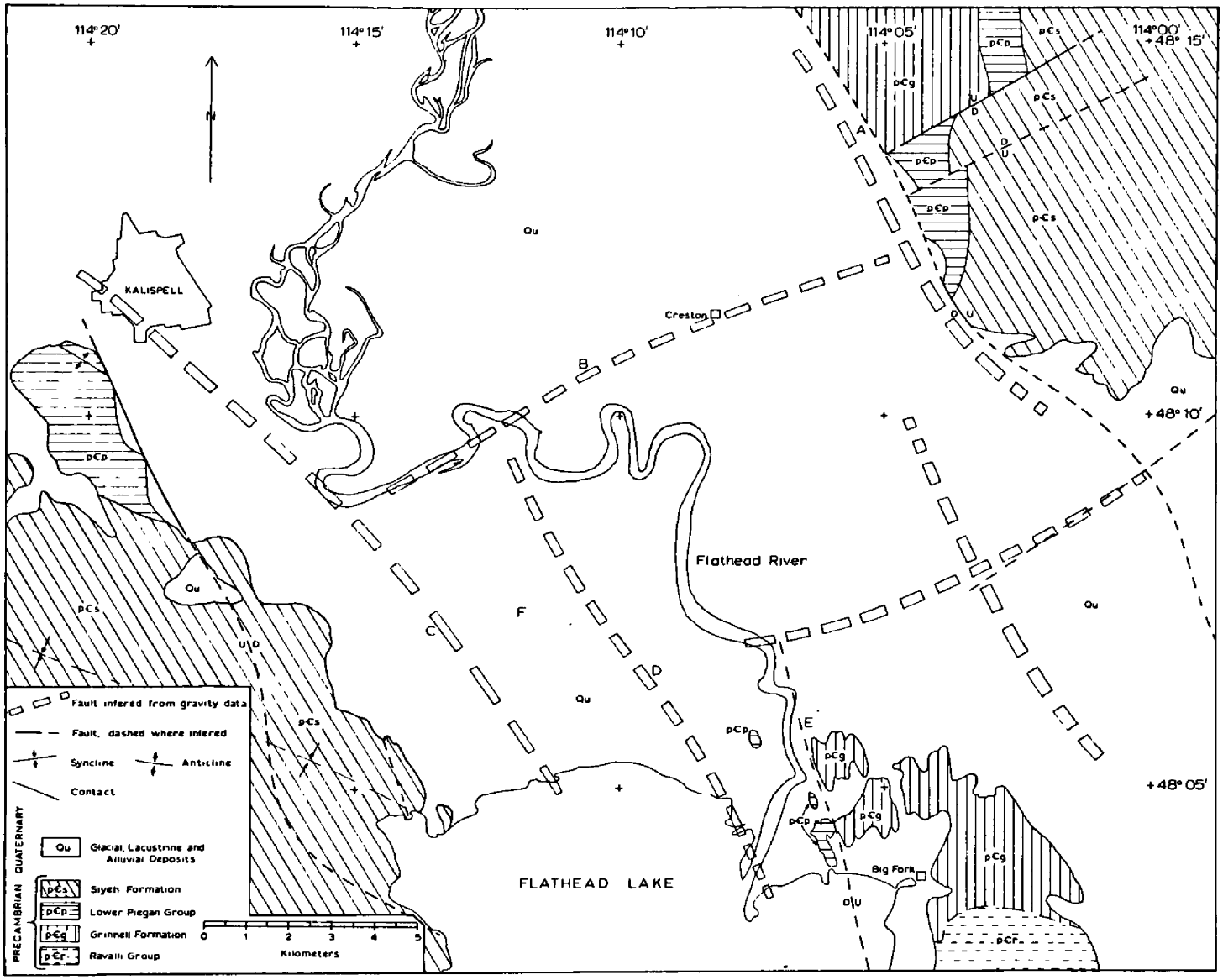

Figure 16. Geologic map of the study area modified from Johns (1970) and faults inferred from gravity data (wide dashed lines). Letters indicate the following features: A - Swan Fault, B - Creston fault, C - Kalispell fault, D and E - splays of the Mission Fault, and F - Flathead graben.

the epicentral distances indicated by the S-P times at HHM. A five kilometer shift to the northwest would also place the epicenters directly over the Creston fault zone. Two of the microearthquakes recorded by the temporary network during 1976 also recorded at HHM with S-P intervals of 2.5 seconds. The epicenters of these two microearthquakes lie 2 to 3 kilometers northwest of the epicenters shown in Figure 11, suggesting that a northwestward shift of the epicenters computed by regional stations (epicentral distances of 100 to 300 kilometers) is justified. Note that the amount of the shift exceeds the northwest "uncertainty" of the epicenters shown in Figure 11.

Systematic mislocations of earthquake epicenters have occurred elsewhere in Montana (Qamar and Hawley, 1979) as well as in central California where data from numerous seismograph stations are available (Uhrhammer, 1980). Systematic epicenter mislocations usually result from lateral variations of seismic velocity and structure of the earth's crust (often along fault zones) between earthquake foci and seismograph stations. These variations are not normally considered in the hypocenter location procedure. In the case of the Kalispell Valley earthquakes, the Helena array, the Orofino array, and station MSO lie south of the Montana Lineament, a major zone of crustal weakness (Weidman, 1965), while the Libby array and the Kalispell Valley lie north of it. The suggested three to five kilometer southward shift of the Kalispell Valley epicenters suggests a higher velocity or thinner crust to the south which may result from changes in crustal structure across the Montana Lineament.

Both the gravity data (Fig. 2) and the cross section showing the better located earthquakes (Fig. 12a) suggest that the Creston fault dips very steeply. However, because of hypocenter uncertainty and the paucity of gravity measurements directly over the Creston fault, one should treat this conclusion with caution. Probably a better determination of the dip of the Creston fault comes from the fault plane solution for the magnitude 5.0 earthquake of February 4, 1975 (Fig. 13b). As discussed above, the Creston fault strikes northeast. An increasing thickness of valley fill northward across the Creston fault implies downward displacement on the northwest side of the fault. In view of these data, the northeast trending nodal planes which dip to the northwest in Figure 13 are taken to represent the fault planes and the southeast dipping nodal planes to represent the auxiliary planes. Figure 13c indicates that the dip-slip and left-lateral strike-slip movement occurred on a fault plane which strikes N60E and dips 50NW. The ratio of dip-slip to strike-slip movement was approximately 3 to 1. Figures 13a and 13c suggest similar types of movement but these fault plane solutions lack sufficient first motions to precisely constrain the nodal planes. The composite fault plane solution for seven microearthquakes along the eastern end of the Creston fault (Fig. 15a) indicates a combination of thrust and strike-slip movement; nearly the opposite sense of movement determined for the larger shocks. The microearthquakes result from tiny movements roughly five orders of magnitude smaller than the largest Kalispell Valley earth-

quake. There is a weak suggestion from the distribution of epicenters that the northeast-trending nodal plane represents the fault plane. If so, this fault plane strikes more northerly and dips more steeply than the main shock fault plane, possibly representing minor movement along a second order fault within the Creston fault zone. The fault plane solutions for the larger Kalispell Valley earthquakes (Fig. 13) indicate a northwest-southeast direction for the axis of minimum compressive stress. Sbar and others (1972) and Stevenson (1976) also determined a predominantly northwest-southeast direction of least compressive stress for microearthquakes occurring in the western Flathead Valley. In contrast to these results, Friedline and others (1976) and Stickney (1977) determined northeast-southwest axes of minimum compressive stress for earthquakes along the Intermountain Seismic Belt in central western Montana. These results suggest a 90 degree rotation of the direction of minimum compressive stress between northwestern and central western Montana across the Montana Lineament.

All of the microearthquakes (Fig. 14) and the better located earthquakes (within the limits of estimated error) shown in Figure 11 fall within the Kalispell Valley. The confinement of earthquakes occurring along the Creston fault to the Kalispell Valley suggests that the Creston fault exists only within the Kalispell Valley. If so, the Creston fault must end where it meets the Swan Fault on the northeast side of the valley and where it meets the Kalispell fault on the southwest side of the valley. The extent of the fault based on gravity

data supports this conclusion. If the Creston fault does transect the Kalispell fault, it has not produced enough offset on the Kalispell fault scarp to produce an obvious signature on the Bouguer gravity map (Fig. 2).

Johns (1970) mapped two parallel normal faults near Trail Creek and Mill Creek which form a small graben structure trending N60E into the Swan Range. The two faults intersect and possibly offset the Swan Fault five kilometers northeast of Creston. During October of 1979, D. Winston and I went into the field to check the relationship between the two northeast trending faults and the Swan Fault. Poor bedrock exposure exists on the lower reaches of the Swan Range near Trail Creek because of thick vegetation and glacial deposits. We nevertheless convinced ourselves that the northeast trending faults exist and that Johns' interpretation of the relative motion along them seemed reasonable. We could not find cross cutting relationships between any of the faults because talus and glacial deposits cover the Swan Fault at the foot of the Swan Range. We found no evidence to suggest recent offset along either northeast trending fault. The gravity map in Figure 2 suggests that the Creston fault ends close to the points where the northeast trending faults intersect the Swan Fault. The northeast trending faults in the Swan Range and the Creston fault may have formed along a common zone of weakness. The lack of evidence of recent faulting and the apparent lack of earthquake activity along the northeast trending faults in the Swan

Mountains suggest that the oblique-slip occurring along the Creston fault does not involve the faults in the Swan Range. If movement is not occurring within the Swan Range, then movement must occur along the Swan Fault to compensate for dip-slip and left-lateral strike-slip movement observed along the Creston fault. The character of the Swan Range front changes from north to south as noted by Davis (1920). North of 48 degrees 13' latitude, steep truncated ridge-spurs or facets run along the base of the Swan Range. The facets have steep slopes of 60 degrees or more and consist of intensely jointed and fractured bedrock. The facets reach a maximum height of 200 to 300 meters above the valley floor and decrease to about 150 meters at their southernmost location just north of Trail Creek (about 48 degrees 13' latitude). Stream drainages have not dissected the Swan Range as deeply to the north of Trail Creek as they have further south. Davis believed that glacial scouring during the last ice age over-steepened the base of the Swan Range and produced the facets. He goes on to say:

> "If faulting is the cause of the truncated spurs, it must be recent and of much smaller amount than that which formed the Swan Range. Recently renewed faulting as an origin for the spur-end facets is therefore improbable, for it can hardly be imagined that renewed faulting of an ancient fault line should terminate southward at just that part of a mountain front where the moraine of a great glacier, which decreased in breadth towards its end, withdrew from the mountain base."

During our field investigation, D. Winston and I found glacial deposits at an elevation of about 1520 meters in the Swan Range, at least 550 meters above the floor of the Kalispell Valley. Alden (1953) estimated a thickness of ice of at least 760 meters in the Kalispell Valley during the last ice age. I would, therefore, expect to find facets carved by glaciers to a greater height than 300 meters above the valley floor. Although glaciers moving down the Rocky Mountain Trench have undoubtedly modified the front of the Swan Range, I suggest that movement along the Swan Fault north of 48 degrees 13' latitude accounts for much of the oversteepened topographic profile along the base of the Swan Range. Konizeski (1968) also believes that faulting is responsible for oversteepening along the base of the Swan Range north of Lake Blaine. He cites several lines of evidence to support his statement, which include: 1) Ice scouring and beveling on the tops of the facets but not on the lower parts of the facets; 2) The facets are part of a regionally uniform joint system along which slickensides clearly indicate movement; and 3) Large talus accumulation at the bases of the facets suggest formation of the facets after glaciation. Although one can refute some of these reasons, several different lines of evidence point to the same conclusion, that dip-slip movement along the northern part of the Swan Fault has occurred in the recent past. Although outside the temporary seismic network, one microearthquake on August 30, 1979 occurred in the Swan Range, just east of the Kalispell Valley, indicating active

faulting in the northern Swan Range. The three first motions observed for this earthquake are compatible with a northward trending normal fault.

The Bouguer gravity map (Fig. 2) indicates that the northern end of the Mission Fault trends about N35W and shows about 600 meters of bedrock offset (Fig. 6). Johns (1970), on the basis of limited bedrock outcrops, mapped the Mission Fault trending about N15W and two to three kilometers east of the fault indicated by gravity data. Both faults probably exist, the fault mapped by Johns may represent a splay of the Mission Fault. The locations and fault plane solution of two microearthquakes recorded during 1979 suggest that the northern end of the Mission Fault is presently active. Gravity data suggest that the Creston fault truncates the Mission Fault. The Kalispell fault and the Mission Fault form the Flathead graben which has approximately 700 meters of relief. An exploratory hole drilled several kilometers southeast of Kalispell (probably near the northern end of the Flathead graben) penetrated 450 meters of gravel without reaching bedrock (Johns, 1970, page 156). The bathymetry of northern Flathead Lake reflects the southward extension of the Flathead graben (Moore, 1980).

The character of the Flathead River changes from north to south along the Kalispell Valley. The Flathead River flows southward from Columbia Falls to Kalispell through numerous coalescing channels which suggest a braided stream. At a point about 5 kilometers south-

east of Kalispell, all of the braided channels converge and the Flathead River flows eastward for about 10 kilometers, then south for 10 kilometers through a series of large meanders. At the point where meandering begins, the gradient of the river changes abruptly from 114 centimeters per kilometer north of the point to about 19 centimeters per kilometer south of the point (Konizeski and others, 1968). Konizeski and others do not discuss the reason for the change in gradient of the Flathead River, however, Moore (1980) suggested that a change in the type of sediment through which the river flows could affect the gradient and character of the river. Fine grained delta deposits have accumulated along the north end of Flathead Lake since the last period of glaciation, but their extent remains unknown. I suggest that the abrupt change in river gradient results from movement along the faults which underlie the Cenozoic deposits in the Kalispell Valley. The Creston fault passes under the Flathead River close to the point where the river begins to meander. Upward movement along the southeast side of the Creston fault would tend to decrease the gradient southward along the Kalispell Valley and possibly cause the river to meander. Dip-slip movement along normal faults bounding the Mission Range may cause eastward tilting of the southwestern corner of the Kalispell Valley and thus account for the eastward jog in the Flathead River before it flows into Flathead Lake.

Conclusions

In the Kalispell Valley, the Kalispell and Swan faults bound the Rocky Mountain Trench (see Fig. 16), the dominate structural feature in the region. Gravity data suggest a thickness of 800 to 900 meters of Cenozoic valley-fill deposits in the Kalispell Valley north of Creston. A graben trends northwest from Flathead Lake and contains about 700 meters of Cenozoic deposits. The Creston fault strikes northeast across the Kalispell Valley and marks the northern end of the Mission block. Most earthquakes in the Kalispell Valley result from oblique-slip (northwest side down and left-lateral) along the Creston fault. Gravity data and field observations suggest that the Creston fault exists only within the Kalispell Valley; it does not extend into the mountains on either side. Concurrent dip-slip movement postulated along the northern end of the Swan Fault and oblique-slip observed along the Creston fault suggest that the floor of the Kalispell Valley north of Creston is moving downward and tilting eastward relative to the Mission block. The concentration of earthquake activity along the eastern half of the Creston fault supports this hypothesis. Garland and others (1961) and Thompson (1962) ascribe gravity lows observed along the Rocky Mountain Trench in British Columbia to basins bounded by pairs of normal faults which cut across the trench and down-drop sections of the trench floor. The Rocky Mountain Trench appears to split into two smaller grabens south of the Creston fault. The Flathead graben represents the southwest

branch, the Swan Valley represents the northeast branch. Sparse gravity data obscure the relationship between the Swan Valley and the Creston fault but to the southwest, the Creston fault transects the Flathead graben. Movement along the Creston and Mission faults may slightly tilt the surface of the Kalispell Valley and affect the gradient of the Flathead River.

BIBLIOGRAPHY

Alden, W.C. (1953), Physiography and Glacial Geology of Western Montana and Adjacent Areas; U.S. Geol. Surv. Prof. Pap. 231, 200 p.

Asada, T. and Aldrich, L.T. (1966), Seismic Observations of Explosions in Montana, The Earth Beneath the Continents; Geoph. Mon. 10, Am. Geophys. Un., Washington, D.C., p. 382-390.

Bennett, G.T., Clowes, R.M., and Ellis, R.M. (1975), A Seismic Refraction Survey along the Southern Rocky Mountain Trench, Canada; Bull. Seis. Soc. Am., v. 65, p. 37-54.

Bible, J.L. (1962), Terrain Correction Tables for Gravity; Geophysics, v. 27, no. 5, p. 715-718.

Birch, F. (Ed.) (1942), Handbook of Physical Constants; Geol. Soc. Am. Special Paper 36, p. 7-26.

Bonini, W.E., Smith, R.B., and Hughes, D.W. (1973), Complete Bouguer Gravity Anomaly Map of Montana; Montana Bureau of Mines and Geology Spec. Pub. 62.

Daly, R.A. (1912), Geology of the North American Cordillera at the Forty-Ninth Parallel; Geol. Surv. Can., Mem. 38, 857 p.

Davis, W.M. (1920), Features of Glacial Origin in Montana and Idaho; Annals of the Assn. of Am. Geog., v. 10, p. 75-148.

Dobrin, M.B. (1960), Introduction to Geophysical Prospecting; McGraw-Hill Book Company.

Friedline, R.A., Smith, R.B., and Blackwell, D.D. (1976), Seismicity and Contemporary Tectonics of the Helena, Montana Area; Bull. Seis. Soc. Am., v. 66, p. 81-95.

Garland, G.D., Kanasewich, E.R. and Thompson, T.L. (1961), Gravity Measurements Over the Southern Rocky Mountain Trench Area of British Columbia; Jour. Geophysical Research, v. 66, p. 2495-2505.

Johns, W.M. (1970), Geology and Mineral Deposits of Lincoln and Flathead Counties, Montana; Montana Bureau of Mines and Geology Bull. 79, 182 p.

Konizeski, R.L., Brietkrietz, A. and McMurtrey, R.G. (1968), Geology and Ground Water Resources of the Kalispell Valley, Northwest Montana; Montana Bureau of Mines and Geology Bull. 68, 42 p.

Lahr, J.C. (1979), HYPOELLIPSE: A Computer Program for Determining Local Earthquake Hypocentral Parameters, Magnitude, and First Motion Pattern; U.S.G.S. Open File Report 79-431, 233 p.

Leech, G.B. and others (1960), Fernie (west half), British Columbia; Geol. Surv. Can., Map 11-1960 (with notes).

McCamy, K., and Meyer, R.P. (1964), A correlation method of apparent velocity measurement; J. Geophys. Res., v. 69, p. 691-699.

Meyers, H. and von Hake, C.A. (1976), Earthquake Data File Summary, Key to Geophysical Records No. 5; National Oceanic and Atmospheric Administration, U.S. Department of Commerce.

Meyer, R.P., Steinhart, J.S. and Bonini, W.E. (1961), Montana, 1959. Explosion Studies of Continental Structure; Carnegie Inst. Wash. Pub. 622, Washington, D.C., p. 305-343.

Milne, W.G. (1967), Earthquake Epicenters and Strain Release in Canada; Can. Jour. Earth Sci.; v. 4, p. 797-814.

_____, and Davenport, A.G. (1969), Distribution of Earthquake Risk in Canada; Bull. Seis. Soc. Am., v. 59, no. 2, p. 729-754.

Moore, J.N. (1980), Personal discussion of Research in Progress.

Mudge, M.R. (1970), Origin of the Disturbed Belt in Northwestern Montana; Geol. Soc. America Bull., v. 81, p. 377-392.

Pardee, J.T. (1950), Late Cenozoic Faulting in Western Montana; Geol. Soc. Am. Bull., v. 61, p. 359-406.

Qamar, A.I. and Breuninger, R. (1979), Northern Tier Report No. 4, Earthquake Hazard to the Proposed Northern Tier Pipeline in Montana; Montana Department of Natural Resources and Conservation, Energy Division, Helena, Montana, 54 p.

Qamar, A. and Hawley, B. (1979), Seismic Activity Near the Three Forks Basin, Montana; Bull. Seis. Soc. Am., v. 69, p. 1917-1930.

Richter, C.F. (1958), Elementary Seismology; W.H. Freeman and Co.

Sbar, M.L., Barazangi, M., Dorman, J., Scholz, C.H., and Smith, R.B. (1972), Tectonics of the Intermountain Seismic Belt, Western United States: Microearthquake Seismicity and Composite Fault Plane Solutions; Geol. Soc. Am. Bull., v. 83, p. 13-28.

Schofield, S.J. (1921), The Origin of the Rocky Mountain Trench, British Columbia; Trans. Roy. Soc. Can., 3rd Ser. v. 14, sec. 4, p. 61-97.

Smith, R.B., and Sbar, M.L. (1974), Contemporary Tectonics and Seismicity of the Western United States with Emphasis on the Inter-Mountain Seismic Belt; Bull. Geol. Soc. Am., v. 85, p. 1205-1218.

Spence, G.D., Ellis, R.M., and Clowes, R.M. (1977), Gravity Evidence Against a High-Angle Fault Crossing the Rocky Mountain Trench near Radium, British Columbia; Can. J. Earth Sci., v. 14, p. 25-31.

Stevenson, P.R. (1976), Microearthquakes at Flathead Lake, Montana: A Study Using Atuomatic Earthquake Processing; Bull. Seis. Soc. Am., v. 66, p. 61-80.

Stickney, M.C. (1978), Seismicity and Faulting of Central Western Montana; Northwest Geology, v. 7, p. 1-9.

Talwani, M., Worzel, J.L., and Landisman, M. (1959), Rapid Gravity Computations for Two-dimensional Bodies with Application to the Mendocino Submarine Fracture Zone; J. Geophys. Res., v. 64, no. 1, p. 49-59.

Telford, W.M., Geldart, L.P., Sheriff, R.E., and Keys, D.A. (1976), Applied Geophysics: Cambridge University Press.

Thompson, T.L. (1962), Origin of the Rocky Mountain Trench in Southeastern British Columbia by Cenozoic Block Faulting; Jour. of the Alberta Soc. of Petrol. Geologists, v. 10, no. 7, p. 408-427.

Uhrhammer, R.A. (1980), Observations of the Coyote Lake, California Earthquake Sequence of August 6, 1979; Bull. Seis. Soc. Am., v. 70, p. 559-570.

United States Earthquakes (annual publication 1928-1968), Environmental Science Services Administration and Coast and Geodetic Survey, U.S. Department of Commerce.

Walton, R., Crosby, G.W., and Sayers, J.E. (1972), Crustal Model through the Libby and Dworshak Seismic Arrays; Unpublished Interim Report, 51 p.

Weidman, R.M. (1965), The Montana Lineament; Billings Geol. Soc. 16th Ann. Field Conf. Guidebook, p. 137-143.

Witkind, I.J. (1975), Preliminary Map Showing Known and Suspected Active Faults in Western Montana; U.S.G.S. Open-File Report 75-285.

Woolard, G.P. (1958), Results for a Gravity Control Network at Airports in the United States; Geophysics, v. 23, p. 520-535.

APPENDIX ONE

Table A1 lists the positions and Bouguer gravity values determined for 285 stations in the Kalispell Valley during the summer of 1979. Following is a brief description of the column headings.

STA NO.	Refrence number of a gravity station.
LAT.	Latitude of a gravity station in decimal degrees.
LONG.	Longitude of a gravity station in decimal degrees.
ELEV.	Elevation above sea level (feet) of a gravity station.
GRAVITY OBSERVED	The observed gravity relative to the Kalispell Airport in milligals.
GRAVITY THEOR.	The theoretical sea-level value of gravity determined from the Gravity Formula 1967 (see Chapter 2).
ELEV. COR.	The elevation correction in milligals (0.09406 x station elevation in ft).
FREE AIR ANOM.	The free air anomaly in milligals (obs. grav. - theor. grav. + elev. corr.)
BOUG. COR.	The Bouguer correction in milligals (-0.03407 x elevation in ft).
BOUG. ANOM.	The Bouguer anomaly in milligals (free air anom. + Bouguer corr.).
TERRAIN CORRECTION	
NEAR	Gravity effect (in milligals) of terrain out ot a distance of 895 meters (through the "F ring" on a Hammer chart) assuming a density of 2.67 grams per cubic centimeter.
FAR	Gravity effect (in milligals) of terrain between 895 meters and 160 kilometers assuming a density of 2.67 grams per cubic centimeter.

COMPLETE BOUGUER ANOMALY — Bouguer gravity anomaly after adding terrain corrections.

Table A1

ACCELERATION OF GRAVITY AT KALISPELL AIRPORT = 980581.9 MILLIGALS.

STA NO.	LAT. (DEG)	LONG. (DEG)	ELEV. FEET	GRAVITY OBSERVED	- THEOR.	+ COR.	=	FREE AIR ANOM.	+	BOUG. COR.	=	BOUG. ANOM.	+	TERRAIN CORRECTION NEAR	FAR	=	COMPLETE BOUGUER ANOMALY
1	48.1026	114.1797	2903.	980582.90	980899.39	273.06		-43.43		-98.91		-142.34		0.00	0.32		-142.02
2	48.1100	114.1797	2902.	980583.61	980900.05	272.96		-43.48		-98.87		-142.35		0.00	0.31		-142.04
3	48.1169	114.1796	2899.	980585.19	980900.67	272.68		-42.81		-98.77		-141.58		0.02	0.31		-141.25
4	48.1243	114.1797	2893.	980587.87	980901.34	272.12		-41.36		-98.56		-139.92		0.02	0.31		-139.59
5	48.1244	114.1667	2893.	980590.38	980901.35	272.59		-38.39		-98.73		-137.12		0.00	0.32		-136.80
6	48.1245	114.1578	2901.	980591.98	980901.36	272.87		-36.51		-98.84		-135.35		0.00	0.34		-135.01
7	48.1209	114.1572	2901.	980591.32	980901.03	272.87		-36.85		-98.84		-135.68		0.00	0.33		-135.35
8	48.1100	114.1580	2897.	980587.24	980900.05	272.49		-40.32		-98.70		-139.02		0.00	0.33		-138.69
9	48.1100	114.1417	2892.	980591.30	980900.05	272.02		-36.72		-98.53		-135.26		0.00	0.36		-134.90
10	48.1027	114.1582	2895.	980584.25	980899.40	272.30		-42.84		-98.63		-141.47		0.00	0.33		-141.14
11	48.0954	114.1583	2896.	980581.93	980898.71	272.40		-44.41		-98.67		-143.08		0.00	0.32		-142.76
12	48.0954	114.1669	2898.	980581.68	980898.74	272.59		-44.47		-98.73		-143.21		0.00	0.32		-142.89
13	48.0951	114.1798	2897.	980582.68	980898.74	272.49		-43.57		-98.70		-142.27		0.00	0.33		-141.94
14	48.0955	114.2011	2907.	980588.21	980898.75	273.43		-37.11		-99.04		-136.15		0.00	0.37		-135.78
15	48.0955	114.2116	2907.	980590.66	980898.75	273.43		-34.66		-99.04		-133.70		0.00	0.40		-133.30
16	48.1062	114.2117	2912.	980589.42	980899.71	273.90		-36.38		-99.21		-135.59		0.00	0.36		-135.23
17	48.1171	114.2117	2901.	980586.95	980900.69	272.67		-40.88		-98.84		-139.72		0.00	0.34		-139.36
18	48.1171	114.2068	2898.	980585.42	980900.69	272.59		-42.68		-98.73		-141.42		0.00	0.33		-141.09
19	48.1245	114.2068	2906.	980585.18	980901.34	273.34		-42.82		-99.01		-141.83		0.00	0.30		-141.53
20	48.1313	114.2067	2904.	980585.04	980901.97	273.15		-43.78		-98.94		-142.72		0.00	0.30		-142.42
21	48.1389	114.2066	2906.	980585.23	980902.65	273.34		-44.09		-99.01		-143.10		0.00	0.29		-142.81
22	48.1390	114.1964	2901.	980588.18	980902.66	272.87		-41.62		-98.84		-140.45		0.00	0.29		-140.16
23	48.1391	114.1793	2904.	980592.96	980902.67	273.15		-36.56		-98.94		-135.50		0.00	0.31		-135.19
24	48.1317	114.1795	2900.	980590.54	980902.01	272.77		-38.69		-98.80		-137.50		0.00	0.31		-137.19
25	48.1244	114.1906	2910.	980585.28	980901.35	273.71		-42.36		-99.14		-141.50		0.02	0.30		-141.18
26	48.1262	114.1578	2898.	980592.32	980901.51	272.59		-36.61		-98.73		-135.34		0.00	0.34		-135.00
27	48.1318	114.1578	2899.	980592.45	980902.02	272.68		-36.89		-98.77		-135.66		0.00	0.35		-135.31
28	48.1392	114.1578	2896.	980594.23	980902.68	272.40		-36.06		-98.67		-134.72		0.00	0.37		-134.35
29	48.1463	114.1576	2896.	980594.96	980903.05	272.40		-35.69		-98.67		-134.36		0.00	0.37		-133.99
30	48.1391	114.1684	2904.	980593.20	980902.67	273.15		-36.33		-98.94		-135.27		0.00	0.33		-134.94
31	48.1462	114.1791	2903.	980593.25	980903.31	273.06		-37.01		-98.91		-135.91		0.00	0.31		-135.60
32	48.1462	114.2060	2901.	980595.30	980903.31	272.97		-45.14		-99.04		-143.98		0.00	0.29		-143.69
33	48.1534	114.2059	2902.	980596.60	980903.96	272.96		-44.40		-98.87		-143.27		0.00	0.29		-142.98

34	48.1506	114.2006	2897.	980587.42	980904.00	272.49	-44.68	-98.70	-143.39	0.00	0.32	-143.07
35	48.1389	114.2221	2895.	980587.69	980902.65	272.30	-42.66	-98.63	-141.29	0.00	0.31	-140.98
36	48.1269	114.2112	2907.	980585.67	980902.65	273.43	-43.55	-99.04	-142.59	0.00	0.29	-142.30
37	48.1171	114.2225	2910.	980589.24	980900.69	273.71	-37.15	-99.14	-136.29	0.00	0.37	-135.92
38	48.1209	114.2334	2911.	980591.30	980901.03	273.81	-35.92	-99.18	-135.10	0.00	0.39	-134.71
39	48.1222	114.2441	2908.	980593.13	980901.15	273.53	-34.50	-99.08	-133.58	0.00	0.42	-133.16
40	48.1136	114.2442	2911.	980593.35	980900.38	273.81	-33.21	-99.18	-132.39	0.00	0.46	-131.93
41	48.1064	114.2442	2909.	980592.93	980899.73	273.62	-33.18	-99.11	-132.29	0.00	0.50	-131.79
42	48.0990	114.2442	2922.	980594.48	980899.06	274.84	-29.74	-99.55	-129.30	0.23	0.53	-129.54
43	48.0955	114.2364	2915.	980593.78	980898.75	274.18	-30.78	-99.31	-130.09	0.17	0.52	-129.40
44	48.0953	114.2226	2913.	980591.50	980898.73	274.00	-33.23	-99.25	-132.48	0.11	0.46	-131.91
45	48.0754	114.2228	2909.	980593.56	980896.94	273.62	-29.74	-99.11	-128.85	0.00	0.57	-128.28
46	48.0865	114.2114	2908.	980591.11	980897.94	273.53	-33.30	-99.08	-132.38	0.00	0.43	-131.95
47	48.1566	114.1500	2899.	980591.92	980904.43	272.68	-39.83	-98.77	-138.60	0.00	0.45	-138.15
48	48.0954	114.1473	2897.	980584.61	980898.74	272.49	-41.64	-98.70	-140.34	0.00	0.33	-140.01
49	48.0882	114.1473	2891.	980581.99	980898.09	271.93	-44.17	-98.50	-142.67	0.00	0.34	-142.33
50	48.0917	114.1312	2901.	980590.03	980898.41	272.87	-35.51	-98.84	-134.34	0.00	0.36	-133.98
51	48.0916	114.1203	2900.	980592.36	980898.41	272.77	-33.28	-98.80	-132.09	0.00	0.40	-131.68
52	48.0945	114.1056	2958.	980588.05	980898.66	279.17	-31.44	-101.12	-132.56	0.27	0.42	-131.87
53	48.1463	114.2222	2903.	980587.05	980903.32	272.96	-43.30	-98.87	-142.18	0.00	0.29	-141.89
54	48.1463	114.2439	2905.	980589.96	980903.32	273.24	-40.12	-98.97	-139.09	0.00	0.32	-138.77
55	48.1463	114.2646	2902.	980595.59	980903.32	272.96	-34.77	-98.87	-133.64	0.00	0.38	-133.26
56	48.1624	114.2551	2908.	980593.19	980904.77	273.53	-38.06	-99.08	-137.13	0.01	0.30	-136.82
57	48.1643	114.2761	2916.	980593.95	980904.94	274.28	-36.71	-99.35	-136.06	0.00	0.31	-135.75
58	48.1644	114.2869	2926.	980594.19	980904.95	275.22	-35.54	-99.69	-135.23	0.00	0.32	-134.91
59	48.1603	114.2676	2929.	980594.65	980904.58	275.50	-34.23	-99.79	-134.02	0.00	0.34	-133.68
60	48.1500	114.2667	2918.	980597.21	980903.65	274.47	-31.97	-99.42	-131.39	0.00	0.39	-131.00
61	48.1442	114.2836	2915.	980596.92	980903.13	274.18	-32.02	-99.31	-131.34	0.00	0.44	-130.90
62	48.1363	114.2760	2905.	980596.94	980903.32	273.24	-33.14	-98.97	-132.11	0.00	0.41	-131.70
63	48.1356	114.2439	2901.	980591.62	980902.36	272.87	-37.87	-98.84	-136.71	0.00	0.38	-136.33
64	48.1281	114.2443	2901.	980593.30	980901.68	272.87	-35.51	-98.84	-134.35	0.00	0.41	-133.94
65	48.1171	114.2543	2911.	980595.57	980900.69	273.81	-31.31	-99.18	-130.49	0.07	0.49	-129.93
66	48.1246	114.2601	2910.	980595.94	980901.37	273.71	-31.72	-99.14	-130.86	0.12	0.49	-130.25
67	48.1308	114.2659	2916.	980595.51	980901.93	274.28	-32.14	-99.35	-131.48	0.01	0.45	-131.02
68	48.1354	114.2616	2914.	980596.80	980902.34	274.09	-31.45	-99.28	-130.73	0.06	0.49	-130.18
69	48.1392	114.2816	2915.	980596.78	980902.68	274.18	-31.71	-99.31	-131.03	0.04	0.47	-130.52
70	48.1391	114.3026	3025.	980592.78	980902.67	284.53	-25.36	-103.06	-128.42	0.75	0.46	-127.21
71	48.1349	114.3002	3063.	980591.05	980902.29	288.11	-23.13	-104.36	-127.49	0.35	0.44	-126.70
72	48.1299	114.2991	3098.	980588.17	980901.84	291.40	-22.27	-105.55	-127.82	0.10	0.45	-127.27
73	48.1282	114.3172	3175.	980583.83	980901.69	298.64	-19.22	-108.17	-127.39	1.19	0.43	-125.77
74	48.1294	114.3253	3407.	980570.01	980901.03	320.46	-10.56	-116.08	-126.63	0.91	0.36	-125.36

75	48.1661	114.3259	3538.	980581.45	980909.77	312.78	-5.50	-120.54	-126.04	0.10	0.37	-124.91
76	48.1536	114.3063	2932.	980598.85	980903.98	275.76	-29.34	-99.89	-129.24	0.10	0.44	-128.76
77	48.1717	114.3086	2936.	980598.22	980905.61	276.16	-31.22	-100.03	-131.25	0.00	0.33	-130.92
78	48.1644	114.3064	2917.	980599.61	980904.95	274.37	-30.97	-99.38	-130.35	0.00	0.39	-129.96
79	48.1608	114.3064	2926.	980599.61	980904.63	275.22	-29.80	-99.69	-129.49	0.00	0.39	-129.10
80	48.1600	114.3039	2934.	980599.72	980904.55	275.97	-28.87	-99.96	-128.83	0.00	0.38	-128.45
81	48.1372	114.3233	3286.	980579.33	980902.50	309.08	-14.10	-111.95	-126.05	0.69	0.37	-124.99
82	48.1450	114.3338	3310.	980579.32	980903.20	311.34	-12.55	-112.77	-125.32	0.47	0.27	-124.58
83	48.1499	114.3408	3315.	980579.54	980903.64	311.81	-12.29	-112.94	-125.24	0.24	0.24	-124.76
84	48.1497	114.3511	3352.	980578.07	980903.63	315.29	-10.27	-114.20	-124.47	0.14	0.22	-124.11
85	48.1461	114.3512	3389.	980575.05	980903.30	318.77	-9.49	-115.46	-124.95	0.33	0.23	-124.39
86	48.1520	114.3514	3324.	980579.19	980903.83	312.66	-11.99	-113.25	-125.24	0.11	0.23	-124.90
87	48.1559	114.3514	3325.	980579.67	980904.18	312.75	-11.76	-113.28	-125.05	0.14	0.23	-124.68
88	48.1587	114.3512	3311.	980579.94	980904.44	311.43	-13.07	-112.81	-125.88	0.12	0.21	-125.55
89	48.1729	114.3368	3575.	980563.93	980905.71	336.26	-5.52	-121.80	-127.32	0.37	0.19	-126.76
90	48.1704	114.3611	3305.	980581.83	980905.49	310.87	-12.79	-112.60	-125.40	0.12	0.20	-125.03
91	48.1857	114.3540	2998.	980600.68	980906.87	281.99	-24.19	-102.14	-126.34	0.08	0.31	-125.95
92	48.1858	114.3397	2943.	980602.07	980906.88	276.82	-27.99	-100.27	-128.25	0.16	0.32	-127.77
93	48.1858	114.3335	2946.	980599.94	980906.88	277.10	-29.84	-100.37	-130.21	0.05	0.30	-129.86
94	48.1825	114.3190	2926.	980598.93	980906.58	275.22	-32.43	-99.69	-132.12	0.00	0.30	-131.82
95	48.1894	114.1578	2960.	980581.10	980907.20	278.42	-47.68	-100.85	-148.53	0.00	0.54	-147.99
96	48.1919	114.1580	2913.	980586.62	980906.52	274.00	-45.91	-99.25	-145.15	0.00	0.52	-144.63
97	48.1749	114.1581	2901.	980587.70	980905.89	272.87	-45.33	-98.84	-144.17	0.00	0.48	-143.69
98	48.1685	114.1635	2903.	980589.12	980905.32	273.06	-43.15	-98.91	-142.05	0.00	0.43	-141.62
99	48.1676	114.1527	2898.	980587.48	980905.24	272.59	-45.18	-98.73	-143.91	0.00	0.48	-143.43
100	48.1748	114.1689	2904.	980588.75	980905.89	273.15	-43.99	-98.94	-142.93	0.00	0.42	-142.51
101	48.1822	114.1761	2951.	980582.44	980906.55	277.57	-46.54	-100.54	-147.08	0.11	0.38	-146.59
102	48.1894	114.1797	2941.	980582.33	980907.20	276.63	-48.24	-100.20	-148.44	0.04	0.40	-148.00
103	48.1965	114.1797	2963.	980580.79	980907.85	278.70	-48.36	-100.95	-149.30	0.02	0.42	-148.85
104	48.1966	114.1906	2964.	980580.77	980907.85	278.79	-48.29	-100.98	-149.27	0.00	0.36	-148.91
105	48.1966	114.2005	2963.	980580.49	980907.85	278.70	-48.65	-100.95	-149.60	0.00	0.32	-149.28
106	48.1855	114.2006	2959.	980580.37	980906.88	278.32	-48.19	-100.81	-149.00	0.00	0.30	-148.70
107	48.1786	114.2006	2952.	980580.84	980906.23	277.67	-47.73	-100.57	-148.30	0.08	0.28	-147.94
108	48.1678	114.2006	2901.	980583.47	980905.26	272.87	-48.92	-98.84	-147.76	0.02	0.30	-147.44
109	48.1606	114.1902	2898.	980586.00	980904.61	272.59	-46.02	-98.73	-144.76	0.00	0.31	-144.45
110	48.1749	114.1906	2899.	980584.91	980905.89	272.68	-48.31	-98.77	-147.08	0.00	0.34	-146.74
111	48.1780	114.2128	2953.	980580.11	980906.17	277.76	-48.31	-100.61	-148.92	0.00	0.25	-148.67
112	48.1859	114.2223	2956.	980580.66	980906.88	278.04	-48.19	-100.71	-148.90	0.07	0.24	-148.59
113	48.1752	114.2277	2907.	980581.22	980905.92	273.43	-51.27	-99.04	-150.31	0.00	0.26	-150.05
114	48.1679	114.2278	2902.	980581.26	980905.26	272.96	-51.05	-98.67	-149.92	0.01	0.25	-149.65
115	48.1536	114.2439	2901.	980586.68	980903.98	272.87	-44.43	-98.64	-143.27	0.00	0.30	-142.97

116	48.1961	114.2495	2902.	980585.17	980905.28	272.96	-47.15	-98.87	-146.02	0.00	0.27	-145.75
117	48.1680	114.2383	2909.	980582.29	980905.27	273.62	-49.37	-99.11	-148.48	0.00	0.26	-148.22
118	48.1752	114.2383	2907.	980581.94	980905.02	273.43	-50.55	-99.04	-149.60	0.00	0.25	-149.35
119	48.1937	114.2489	2908.	980583.63	980907.59	273.53	-50.44	-99.08	-149.51	0.01	0.24	-149.26
120	48.2008	114.2492	2906.	980584.19	980908.23	273.34	-50.70	-99.01	-149.71	0.00	0.24	-149.47
121	48.2004	114.2312	2924.	980584.19	980908.19	275.03	-48.97	-99.62	-148.59	0.03	0.26	-148.30
122	48.1966	114.1581	2966.	980578.53	980907.85	278.98	-50.33	-101.05	-151.38	0.00	0.59	-150.79
123	48.1966	114.1689	2961.	980579.73	980907.85	278.51	-49.61	-100.88	-150.49	0.00	0.50	-149.99
124	48.2038	114.1689	2972.	980578.17	980908.50	279.55	-50.73	-101.26	-152.03	0.00	0.54	-151.49
125	48.1653	114.2114	2961.	980580.09	980906.88	278.51	-48.28	-100.88	-149.16	0.00	0.26	-148.90
126	48.1967	114.2222	2957.	980582.84	980907.86	276.25	-48.76	-100.06	-148.83	0.00	0.26	-148.57
127	48.1967	114.2114	2945.	980582.19	980907.86	277.01	-48.66	-100.34	-149.00	0.00	0.29	-148.71
128	48.2038	114.2006	2922.	980583.83	980908.50	274.84	-49.32	-99.55	-148.88	0.00	0.36	-148.52
129	48.2111	114.2005	2934.	980583.16	980909.15	275.97	-50.03	-99.96	-149.99	0.00	0.39	-149.60
130	48.2111	114.1906	2925.	980582.35	980909.15	275.13	-51.68	-99.65	-151.33	0.00	0.45	-150.88
131	48.2112	114.1784	2974.	980577.65	980909.16	279.73	-51.79	-101.32	-153.10	0.02	0.51	-152.57
132	48.2111	114.1680	2974.	980576.53	980909.15	279.73	-52.89	-101.32	-154.21	0.00	0.60	-153.61
133	48.2111	114.1581	2973.	980575.55	980909.15	279.64	-53.96	-101.29	-155.26	0.00	0.71	-154.55
134	48.2039	114.1580	2970.	980576.80	980908.50	279.36	-52.35	-101.19	-153.54	0.00	0.65	-152.89
135	48.2184	114.1581	2976.	980574.58	980909.81	279.92	-55.31	-101.39	-156.70	0.00	0.79	-155.91
136	48.2256	114.1581	2980.	980574.41	980910.46	280.30	-55.75	-101.53	-157.28	0.00	0.88	-156.40
137	48.2260	114.1674	2977.	980574.32	980910.49	280.02	-56.16	-101.43	-157.58	0.00	0.75	-156.83
138	48.2259	114.1854	2965.	980576.62	980910.48	278.89	-54.98	-101.02	-155.99	0.00	0.56	-155.43
139	48.2104	114.2554	2929.	980583.11	980909.09	275.50	-50.48	-99.79	-150.27	0.06	0.21	-150.00
140	48.1970	114.2545	2905.	980583.78	980907.88	273.24	-50.86	-98.97	-149.83	0.00	0.22	-149.61
141	48.2111	114.2266	2932.	980583.72	980909.15	275.78	-49.65	-99.89	-149.55	0.00	0.27	-149.28
142	48.2111	114.2112	2926.	980583.82	980909.15	275.41	-49.93	-99.76	-149.68	0.00	0.34	-149.34
143	48.2174	114.2223	2933.	980583.55	980909.72	275.68	-50.30	-99.93	-150.22	0.00	0.31	-149.91
144	48.2210	114.2005	2933.	980580.88	980910.04	275.88	-53.29	-99.93	-153.22	0.08	0.43	-152.71
145	48.2111	114.1473	2969.	980575.49	980909.15	279.26	-54.39	-101.15	-155.55	0.00	0.86	-154.69
146	48.2111	114.1364	2966.	980576.19	980909.15	278.98	-53.93	-101.05	-155.03	0.00	1.05	-153.98
147	48.2038	114.1363	2959.	980577.02	980908.50	278.32	-53.16	-100.81	-153.97	0.00	0.93	-153.04
148	48.1894	114.1472	2954.	980579.48	980907.20	277.85	-49.87	-100.64	-150.51	0.00	0.63	-149.88
149	48.1895	114.1362	2954.	980580.30	980907.21	277.85	-49.05	-100.64	-149.70	0.00	0.75	-148.95
150	48.1533	114.1366	2906.	980589.16	980903.95	273.34	-41.46	-99.01	-140.47	0.00	0.50	-139.97
151	48.1461	114.1366	2899.	980590.48	980903.30	272.68	-40.15	-98.77	-138.92	0.00	0.47	-138.45
152	48.1355	114.1366	2898.	980589.00	980902.35	272.59	-40.76	-98.73	-139.50	0.00	0.43	-139.07
153	48.1518	114.1366	2900.	980589.18	980902.02	272.77	-40.06	-98.80	-138.87	0.00	0.42	-138.45
154	48.1247	114.1148	2898.	980588.59	980901.38	272.59	-40.20	-98.73	-138.94	0.00	0.50	-138.44
155	48.1283	114.1038	2955.	980582.52	980901.70	277.95	-41.24	-100.68	-141.92	0.00	0.53	-141.39
156	48.1248	114.0944	2970.	980581.25	980901.39	279.36	-40.78	-101.19	-141.96	0.00	0.55	-141.41

157	48.1994	114.1942	2986.	980579.56	980901.71	280.56	-49.69	-101.73	-142.62	0.02	0.59	-142.01
158	48.1894	114.1966	3039.	980576.54	980902.70	285.75	-48.40	-103.50	-143.91	0.14	0.56	-143.21
159	48.2330	114.1958	2972.	980575.49	980911.12	279.55	-56.08	-101.26	-157.34	0.17	0.50	-156.67
160	48.2402	114.1961	2984.	980573.91	980911.77	280.68	-57.19	-101.66	-158.86	0.00	0.53	-158.33
161	48.2401	114.2071	3006.	980574.78	980911.76	282.74	-54.24	-102.41	-156.65	0.02	0.42	-156.21
162	48.2474	114.1960	2982.	980573.61	980912.42	280.49	-58.32	-101.60	-159.92	0.01	0.57	-159.34
163	48.2475	114.1853	2980.	980573.61	980912.43	280.30	-58.52	-101.53	-160.05	0.00	0.70	-159.35
164	48.2403	114.1853	2984.	980573.70	980911.78	280.68	-57.41	-101.66	-159.08	0.00	0.65	-158.43
165	48.2331	114.1853	2971.	980575.53	980911.13	279.45	-56.15	-101.22	-157.37	0.00	0.60	-156.77
166	48.2329	114.1838	2983.	980574.00	980911.11	280.58	-56.54	-101.63	-158.17	0.00	0.87	-157.30
167	48.2401	114.1836	2992.	980573.02	980911.76	281.43	-57.32	-101.94	-159.25	0.00	0.98	-158.27
168	48.2401	114.1531	3004.	980572.84	980911.76	282.56	-56.37	-102.35	-158.72	0.00	1.16	-157.56
169	48.2474	114.1536	3000.	980573.29	980912.42	282.18	-56.95	-102.21	-159.16	0.00	1.08	-158.08
170	48.2511	114.1535	3034.	980571.43	980912.75	285.38	-55.95	-103.37	-159.32	0.00	1.08	-158.24
171	48.2511	114.1529	3020.	980572.57	980912.75	284.06	-56.12	-102.89	-159.01	0.00	1.35	-157.66
172	48.2511	114.1420	3038.	980572.68	980912.75	285.75	-54.31	-103.50	-157.82	0.00	1.56	-156.26
173	48.2483	114.1366	3013.	980574.17	980912.50	283.40	-54.92	-102.65	-157.57	0.00	1.58	-155.99
174	48.2401	114.1311	3075.	980569.79	980911.76	289.23	-52.74	-104.77	-157.50	0.00	1.46	-156.04
175	48.2329	114.1311	3057.	980570.58	980911.11	287.54	-53.00	-104.15	-157.15	0.00	1.48	-155.67
176	48.2111	114.2861	2918.	980588.21	980909.15	274.47	-46.47	-99.42	-145.89	0.02	0.20	-145.67
177	48.2045	114.2989	2942.	980588.91	980908.56	276.72	-42.93	-100.23	-143.16	0.08	0.20	-142.88
178	48.1996	114.3116	2955.	980590.20	980908.12	277.95	-39.98	-100.66	-140.65	0.00	0.22	-140.43
179	48.2007	114.3269	2958.	980593.01	980909.22	278.23	-36.93	-100.78	-137.76	0.00	0.24	-137.52
180	48.1969	114.3401	2964.	980594.33	980907.87	278.79	-34.75	-100.98	-135.73	0.00	0.27	-135.46
181	48.1972	114.3547	3084.	980588.43	980907.90	290.08	-29.39	-105.07	-134.47	0.14	0.21	-134.12
182	48.1972	114.3723	3042.	980593.18	980907.90	286.13	-28.59	-103.64	-132.23	0.06	0.28	-131.89
183	48.1896	114.3728	3058.	980594.10	980907.22	287.64	-25.48	-104.19	-129.67	0.11	0.31	-129.25
184	48.1888	114.3617	3046.	980593.73	980907.15	286.51	-26.91	-103.78	-130.69	0.02	0.28	-130.39
185	48.1867	114.3084	2938.	980592.12	980906.96	276.35	-38.49	-100.10	-138.59	0.00	0.26	-138.33
186	48.1916	114.2966	2932.	980599.75	980906.50	275.78	-40.97	-99.89	-140.86	0.00	0.27	-140.59
187	48.1825	114.2869	2939.	980597.38	980906.58	276.44	-42.76	-100.13	-142.89	0.00	0.24	-142.65
188	48.1933	114.2897	2909.	980589.33	980907.55	273.62	-44.61	-99.11	-143.71	0.00	0.24	-143.47
189	48.1978	114.2870	2909.	980588.80	980907.96	273.62	-45.53	-99.11	-144.64	0.00	0.23	-144.41
190	48.2003	114.2918	2904.	980589.85	980908.18	273.53	-44.81	-99.08	-143.88	0.01	0.23	-143.64
191	48.2079	114.2739	2908.	980585.54	980908.86	273.53	-49.80	-99.08	-148.88	0.00	0.22	-148.66
192	48.2087	114.2655	2914.	980583.88	980908.94	274.09	-50.97	-99.28	-150.25	0.00	0.22	-150.03
193	48.2189	114.2664	2918.	980583.64	980909.95	274.47	-51.74	-99.42	-151.16	0.00	0.21	-150.95
194	48.2242	114.2541	2920.	980583.29	980910.33	274.66	-52.39	-99.48	-151.87	0.00	0.23	-151.64
195	48.2210	114.2400	2990.	980578.75	980910.04	281.24	-50.05	-101.87	-151.92	0.55	0.22	-151.15
196	48.2256	114.1365	3058.	980569.20	980910.46	287.64	-53.63	-104.19	-157.82	0.00	1.18	-156.64
197	48.2256	114.1311	3064.	980569.07	980910.46	288.20	-53.13	-104.39	-157.57	0.00	1.30	-156.27

198	48.2113	114.1233	3001.	980569.30	980911.73	269.60	-52.68	-104.97	-157.65	0.05	1.67	-155.93
199	48.2256	114.1147	3044.	980571.24	980910.46	256.32	-52.89	-103.71	-156.60	0.00	1.64	-154.96
200	48.2163	114.1147	3036.	980570.45	980909.80	265.67	-53.79	-103.44	-157.23	0.00	1.51	-155.72
201	48.2114	114.1147	3018.	980571.21	980909.18	283.37	-54.09	-102.82	-156.92	0.00	1.41	-155.51
202	48.2114	114.1039	3016.	980572.05	980909.18	283.68	-53.44	-102.76	-156.19	0.00	1.58	-154.61
203	48.2064	114.0896	3007.	980575.47	980908.73	292.84	-50.42	-102.45	-152.87	0.06	1.78	-151.03
204	48.2038	114.0744	3114.	980573.44	980908.50	292.90	-42.15	-106.09	-148.25	0.26	1.69	-146.30
205	48.2150	114.0770	3196.	980569.88	980909.50	300.80	-38.82	-108.96	-147.78	0.22	1.75	-145.81
206	48.2256	114.0878	3176.	980569.93	980910.46	296.73	-41.79	-109.21	-150.00	0.31	1.65	-148.04
207	48.2256	114.1020	3056.	980572.36	980910.46	287.45	-50.65	-104.12	-154.77	0.00	1.72	-153.05
208	48.2350	114.1056	3014.	980576.07	980911.30	283.50	-51.73	-102.69	-154.42	0.04	1.74	-152.64
209	48.0954	114.0891	3048.	980586.13	980898.74	286.69	-25.92	-103.95	-129.76	0.02	0.46	-129.28
210	48.0957	114.0717	3045.	980587.60	980898.77	286.41	-24.75	-103.74	-128.49	0.07	0.57	-127.85
211	48.0957	114.0606	3064.	980584.14	980898.77	288.20	-26.42	-104.39	-130.81	0.01	0.65	-130.15
212	48.0956	114.0282	3057.	980573.15	980898.76	287.54	-38.07	-104.15	-142.22	0.00	1.04	-141.18
213	48.1023	114.0263	3053.	980570.48	980899.36	287.17	-41.72	-104.02	-145.73	0.00	1.10	-144.63
214	48.1101	114.0284	3056.	980568.41	980900.06	287.45	-44.21	-104.12	-148.33	0.00	1.18	-147.15
215	48.1103	114.0394	3043.	980573.59	980900.08	286.22	-40.27	-103.68	-143.94	0.00	1.01	-142.93
216	48.1103	114.0500	3049.	980579.76	980900.08	286.79	-33.53	-103.88	-137.41	0.00	0.85	-136.56
217	48.1175	114.0683	3077.	980583.80	980900.73	289.42	-27.51	-104.83	-132.34	0.02	0.68	-131.64
218	48.1223	114.0769	3089.	980582.84	980901.16	290.55	-27.77	-105.24	-133.01	0.04	0.62	-132.35
219	48.0811	114.0923	3023.	980588.80	980897.45	284.34	-24.31	-102.99	-127.30	0.25	0.43	-126.62
220	48.0702	114.1083	2996.	980596.37	980896.47	272.40	-27.70	-98.67	-126.37	0.02	0.43	-125.92
221	48.0666	114.1029	2897.	980596.58	980896.15	272.49	-27.08	-98.70	-125.78	0.07	0.45	-125.26
222	48.0667	114.1132	2896.	980594.39	980896.15	272.40	-29.37	-98.67	-128.03	0.00	0.41	-127.62
223	48.0668	114.0922	2931.	980592.71	980896.16	275.69	-27.77	-99.86	-127.62	0.07	0.47	-127.08
224	48.0720	114.0922	2961.	980592.85	980896.63	278.51	-25.27	-100.88	-126.15	0.17	0.46	-125.52
225	48.0753	114.0939	3066.	980586.92	980896.93	288.39	-21.62	-104.46	-126.08	0.19	0.39	-125.50
226	48.1029	114.0819	3049.	980584.97	980899.41	286.79	-27.76	-103.88	-131.64	0.00	0.50	-131.14
227	48.1103	114.0816	3066.	980594.14	980900.08	288.39	-27.55	-104.46	-132.01	0.12	0.54	-131.35
228	48.1030	114.0928	3041.	980586.27	980899.42	286.04	-27.12	-103.61	-130.73	0.00	0.46	-130.27
229	48.1067	114.1111	2948.	980594.75	980899.76	277.29	-27.72	-100.44	-128.16	0.04	0.43	-127.69
230	48.1126	114.1114	2930.	980596.23	980900.29	275.60	-28.47	-99.83	-128.29	0.01	0.45	-127.83
231	48.1066	114.0928	3019.	980587.37	980899.75	283.97	-26.41	-102.56	-131.27	0.01	0.48	-130.78
232	48.1136	114.0930	3061.	980585.77	980900.38	287.92	-26.70	-104.29	-130.99	0.02	0.48	-130.43
233	48.1613	114.1328	2944.	980587.74	980904.67	276.91	-40.01	-100.30	-140.32	0.03	0.54	-139.75
234	48.1661	114.1093	2962.	980590.77	980905.10	278.61	-35.73	-100.92	-136.64	0.04	0.78	-135.82
235	48.1691	114.0847	3079.	980578.63	980905.37	289.61	-37.14	-104.90	-142.04	0.04	1.02	-140.98
236	48.1887	114.1202	2927.	980589.93	980907.14	275.31	-41.89	-99.72	-141.62	0.00	0.98	-140.64
237	48.1969	114.0714	3193.	980568.32	980907.87	300.33	-39.22	-106.79	-148.00	0.13	1.56	-146.31
238	48.1851	114.0505	3267.	980562.92	980906.31	307.29	-36.59	-111.31	-147.90	0.40	1.65	-145.85

239	48.1759	114.0[illegible]	3220.	980568.48	980905.08	302.37	-10.63	-109.71	-150.34	0.03	1.67	-146.74
240	48.1766	114.0288	3375.	980555.83	980905.05	317.15	-32.77	-114.99	-147.75	0.04	2.12	-145.59
241	48.1669	114.0269	3237.	980560.38	980905.17	304.47	-40.33	-110.28	-150.62	0.02	2.06	-148.51
242	48.1539	114.0074	3155.	980563.00	980904.00	296.76	-44.25	-107.49	-151.74	0.02	2.98	-148.74
243	48.1463	114.0072	3111.	980559.72	980903.32	292.62	-50.98	-105.99	-156.98	0.00	2.75	-154.23
244	48.1361	114.0073	3078.	980554.50	980902.40	289.52	-58.09	-104.87	-162.96	0.00	2.38	-160.58
245	48.1679	114.1798	2890.	980587.44	980905.26	271.83	-45.98	-98.46	-144.44	0.00	0.36	-144.08
246	48.1861	114.2331	2956.	980584.19	980906.90	273.34	-49.38	-99.01	-148.39	0.00	0.25	-148.14
247	48.2078	114.2492	2912.	980584.33	980908.86	273.90	-50.62	-99.21	-149.83	0.01	0.23	-149.59
248	48.2184	114.1689	2976.	980575.90	980909.81	279.92	-53.99	-101.39	-155.38	0.00	0.66	-154.72
249	48.1501	114.0966	3047.	980584.21	980903.66	286.60	-32.85	-103.81	-136.66	0.00	0.67	-135.99
250	48.1499	114.0860	3041.	980581.10	980903.64	286.04	-36.50	-103.61	-140.11	0.05	0.65	-139.31
251	48.1436	114.0648	3132.	980571.88	980903.08	294.60	-36.61	-106.71	-143.32	0.03	0.89	-142.40
252	48.1479	114.0473	3047.	980572.60	980903.46	286.60	-44.26	-103.81	-148.07	0.06	1.33	-146.68
253	48.1392	114.0405	3061.	980568.66	980902.68	287.92	-45.91	-104.29	-150.20	0.02	1.32	-148.86
254	48.1303	114.0344	3030.	980568.10	980901.88	285.00	-48.73	-103.23	-152.01	0.03	1.36	-150.62
255	48.1262	114.0234	3076.	980562.46	980901.51	289.33	-49.72	-104.60	-154.52	0.04	1.50	-152.98
256	48.1100	114.0069	3042.	980564.67	980900.05	286.13	-49.25	-103.64	-152.89	0.00	1.75	-151.14
257	48.1172	114.0069	3059.	980563.09	980900.70	287.73	-49.89	-104.22	-154.11	0.00	1.86	-152.25
258	48.1244	114.0072	3069.	980562.45	980901.35	288.67	-50.23	-104.56	-154.79	0.00	2.01	-152.78
259	48.0955	114.0069	3027.	980569.37	980898.75	284.72	-44.66	-103.13	-147.79	0.00	1.54	-146.25
260	48.0957	114.0499	3059.	980580.05	980898.77	287.73	-30.98	-104.22	-135.20	0.01	0.76	-134.43
261	48.0883	114.0496	3064.	980583.40	980898.10	288.20	-26.50	-104.39	-130.89	0.01	0.73	-130.15
262	48.0883	114.0369	3064.	980580.84	980898.10	288.20	-29.06	-104.39	-133.45	0.00	0.85	-132.60
263	48.0883	114.0279	3060.	980577.13	980898.10	287.82	-33.15	-104.25	-137.41	0.00	1.00	-136.41
264	48.0650	114.0814	2971.	980589.97	980896.00	279.45	-26.58	-101.22	-127.80	0.10	0.49	-127.21
265	48.0570	114.0263	3016.	980584.07	980895.28	283.87	-27.34	-102.82	-130.16	0.65	0.89	-128.62
266	48.0664	114.0226	3045.	980582.55	980896.13	286.41	-27.17	-103.74	-130.91	0.38	0.96	-129.57
267	48.0811	114.0278	3057.	980579.61	980897.45	287.54	-30.30	-104.15	-134.45	0.02	0.95	-133.48
268	48.0663	114.0061	3037.	980575.53	980896.12	285.66	-34.92	-103.47	-138.39	0.00	1.26	-137.13
269	48.0518	114.0114	3059.	980579.51	980894.81	287.73	-27.58	-104.22	-131.80	0.01	1.07	-130.72
270	48.0812	114.0706	3167.	980580.11	980897.46	297.89	-19.46	-107.90	-127.36	0.31	0.47	-126.59
271	48.1393	114.2653	2910.	980600.76	980902.69	273.71	-28.22	-99.14	-127.37	0.01	0.42	-126.94
272	48.0898	114.0653	3338.	980567.86	980898.23	313.97	-16.41	-113.73	-130.13	1.27	0.48	-128.38
273	48.0811	114.1069	2900.	980597.89	980897.45	272.77	-26.79	-98.80	-125.59	0.03	0.44	-125.12
274	48.1969	114.1149	2946.	980577.53	980907.37	277.10	-53.24	-100.37	-153.61	0.00	1.19	-152.42
275	48.1934	114.1203	2932.	980579.42	980907.56	275.78	-52.36	-99.89	-152.25	0.00	1.03	-151.22
276	48.1749	114.1310	2893.	980594.61	980905.89	272.59	-38.70	-98.73	-137.43	0.00	0.71	-136.72
277	48.1749	114.1417	2900.	980595.98	980905.89	272.77	-37.14	-98.80	-135.95	0.00	0.58	-135.37
278	48.1822	114.1363	2906.	980594.22	980906.55	273.34	-39.00	-99.01	-138.00	0.04	0.72	-137.24
279	48.1847	114.1141	2940.	980589.32	980906.78	276.54	-40.92	-100.17	-141.08	0.00	1.05	-140.03

280	48.1342	114.1110	2945.	980593.79	980906.73	277.81	-40.93	-100.54	-141.27	0.00	1.16	-140.11
281	48.1742	114.1089	2940.	980891.15	980905.33	276.54	-38.14	-100.17	-138.31	0.06	0.90	-137.35
282	48.1501	114.1093	2955.	980591.34	980903.66	277.95	-34.38	-100.68	-135.06	0.03	0.64	-134.39
283	48.1353	114.2617	2910.	980599.35	980902.33	273.71	-29.27	-99.14	-128.41	0.00	0.43	-127.98
284	48.1392	114.2438	2898.	980596.27	980902.68	272.59	-33.83	-98.73	-132.56	0.00	0.28	-132.28
285	48.1535	114.1150	2944.	980591.92	980903.97	276.91	-35.13	-100.30	-135.43	0.02	0.62	-134.79

APPENDIX TWO

Appendix two contains a listing of the Fortran computer program BOUGER.FOR which was used to compute the complete Bouguer gravity values for gravity stations in the Kalispell Valley. Before using BOUGER.FOR, change the file names in the OPEN statements (lines 110-130) to the names of your data files.

```
00100   C...PROGRAM BOUGER.FOR
00200   C...COMPUTES COMPLETE BOUGUER GRAVITY ANOMALY.  EACH LINE OF INPUT DATA
00300   C...FILE, GRVIN.DAT CONAINS: LATITUDE IN DEGREES(X), LONGITUDE(B),
00400   C...ELEVATION IN FEET(E), A GRAVITY READING IN MILLIGALS(GS), WHICH
00500   C...IS THE DIFFERENCE BETWEEN A MASTER BASE STATION AND A STATION,
00600   C...TERRAIN CORRECTIONS THRU RING F(TCI) AND TERRAIN CORRECTIONS BEYOND
00700   C...RING F(TCO).  OUTPUT DATA FILE NAMED GRVDAT.OUT.  PLOT FILE NAMED
00800   C...GRVDAT.PLT.  RENAME FILE='NAME.***' IN OPEN STATEMENTS FOR YOUR OWN
00900   C...DATA FILES.  MODIFIED NOV, 1979 AND APR, 1980 BY MC STICKNEY.
01000           DOUBLE PRECISION AA,BB,CC,DD,G,D
01100           OPEN(UNIT=6,DEVICE='DSK',ACCESS='SEQIN',FILE='NAME.IN')
01200           OPEN(UNIT=8,DEVICE='DSK',ACCESS='SEQOUT',FILE='NAME.PLT')
01300           OPEN(UNIT=5,DEVICE='DSK',ACCESS='SEQOUT',FILE='NAME.OUT')
01400           DATA AA,BB,CC,DD,N/978031.85,.005278895,.000023462,6.283185307,0/
01500   C...USER ENTERS DATA.
01600           TYPE 10
01700   10      FORMAT(1X,'ENTER GRAVITY (IN MG) OF MASTER BASE STATION:  '$)
01800           ACCEPT 12,BASVAL
01900   12      FORMAT(F)
02000           TYPE 14
02100   14      FORMAT(1X,'DO YOU WANT A PLOTTER FILE CREATED?  '$)
02200           ACCEPT 16,IANSER
02300   16      FORMAT(A5)
02400           WRITE(5,20)BASVAL
02500   20      FORMAT(1X,'ACCELERATION OF GRAVITY AT KALISPELL AIRPORT = '
02600           1F10.1' MILLIGALS'/)
02700   C...WRITE OUT HEADINGS.
02800           WRITE(5,570)
02900   570     FORMAT(58X,'FREE',22X,'TERRAIN  COMPLETE')
03000           WRITE(5,580)
03100   580     FORMAT(1X,'STA   LAT.   LONG.   ELEV.  G R A V I T Y      ',
03200           1'ELEV.     AIR      BOUG.   BOUG.  CORRECTION  BOUGUER')
03300           WRITE(5,600)
```

```
03400    600     FORMAT(1X,'NO.  (DEG)   (DEG)   FEET  OBSERVED - THEOR.
03500            1  + COR.  =  ANOM. +  COR. =  ANOM.+ NEAR+ FAR = ANOMALY')
03600            WRITE(5,610)
03700    610     FORMAT(1X,'--- ------- -------- ----- -------- --------
03800            1------   ------  ------- -------  ----  ----  -------')
03900    C...LOOP READS, PROCESSES AND WRITES A GRAVITY STATION.
04000    100     N=N+1
04100            READ(6,1000,END=800)X,B,E,GS,TCI,TCO
04200    1000    FORMAT(6F)
04300            TERCOR=TCI+TCO
04400            D=X*DD/360
04500            G=AA*(1.+BB*(DSIN(D))**2.+CC*(DSIN(D))**4.)
04600            ELCOR=.09406*E
04700            BCOR=-.03407*E
04800            GRAW=BASVAL+GS
04900            GFA=GRAW+ELCOR-G
05000            GBG=GFA+BCOR
05100            DDD=D*360./DD
05200            TOT=GBG+TERCOR
05300            WRITE(5,700)N,DDD,B,E,GRAW,G,ELCOR,GFA,BCOR,GBG,TCI,TCO,TOT
05400    700     FORMAT(1X,I3,1X,F7.4,1X,F8.4,1X,F5.0,1X,F9.2,1X,F9.2,1X,
05500            1F6.2,2X,F7.2,2X,F7.2,1X,F7.2,1X,F5.2,1X,F5.2,2X,F7.2)
05600            IF(IANSER.NE.'YES  ') GO TO 99
05700            BNEG=-B
05800            GBGN=-TOT
05900            WRITE(8,701)DDD,BNEG,FF1,GBGN
06000    701     FORMAT(1X,F8.4,F10.4,' .075 8 ',F10.2)
06100    99      GO TO 100
06200    800     CALL EXIT
06300            END
```

APPENDIX THREE

Table A2 lists the hypocentral parameters determined by HYPOELLIPSE (Lahr, 1979) for 98 Kalispell Valley earthquakes recroded by the Earthquake Research Lab at the University of Montana. Table A3 contains the hypocentral parameters for 14 Kalispell Valley microearthquakes recorded by temoprary networks of seismograph stations. Following is a brief description of the column headings for Tables A2 and A3. For more detailed descriptions of these parameters see Lahr (1979).

DATE The year, month and day of an earthquake.

ORIGIN The hours, minutes and seconds of the origin time of an earthquake.

LAT N Latitude of an earthquake epicenter in degrees and minutes.

LONG W Longitude of an earthquake epicenter in degrees and minutes.

DEPTH The depth of a hypocenter (in km) below the earth's surface.

MAG Earthquake magnitude determined from WWSSN station MSO.

NO Number of S-P, P- and S-wave arrival times used to locate an earthquake.

GAP The greatest azimuthal gap between seismograph stations used to locate an earthquake.

DMIN Distance from an earthquake epicenter to the closest seismograph station in kilometers.

RMS Root mean square of the travel time residuals in seconds.

ERH Estimate of the standard error in epicentral location (in km) in the direction of maximum uncertainty.

ERZ Estimate of the standard error in the depth of the hypocenter in kilometers.

Q Quality of a hypocenter solution based on the RMS, ERH, ERZ, NO, GAP and DMIN.

TABLE A2

DATE	ORIGIN	LAT N	LONG W	DEPTH	MAG	NO	GAP	DMIN	RMS	ERH	ERZ	Q
740826	1012 48.79	48N 2.82	113W55.73	0.63	1.2	10	189	128.8	0.38	6.0	99.0	D
741225	148 55.38	47N57.67	114W29.75	7.99	1.8	23	90	93.6	0.74	3.4	4.1	D
741225	227 29.38	47N57.94	114W26.78	10.55	2.2	20	93	96.6	0.32	2.1	2.2	D
741225	251 28.81	47N55.98	114W29.32	0.12	1.6	16	91	95.6	0.59	3.3	6.3	D
750116	748 38.72	48N15.07	114W 4.56	18.54	1.5	10	144	102.0	0.59	26.9	15.5	D
750117	1453 59.99	48N 9.34	114W 4.06	0.31	2.7	21	128	109.8	0.71	5.1	5.0	D
750119	142 31.32	48N 9.21	114W 4.32	5.27	2.0	13	129	109.8	0.38	5.9	6.1	D
750120	622 34.51	48N10.70	114W 5.44	11.81	2.1	15	124	106.9	0.50	6.4	5.5	C
750120	854 45.01	48N10.61	114W 2.92	10.76	1.5	8	136	109.2	0.05	1.3	1.2	C
750121	1811 38.28	48N 8.70	114W 7.63	11.59	3.0	14	118	107.6	0.27	3.0	3.2	C
750122	1756 32.14	48N10.32	114W 3.60	1.25	1.8	11	138	109.0	0.30	1.7	1.7	C
750123	1013 58.60	48N 8.98	114W 7.99	0.26	1.6	14	128	107.0	0.64	7.0	99.0	D
750123	1323 57.63	48N 8.27	114W 5.81	4.23	2.7	14	124	109.7	0.46	5.5	9.7	D
750123	16 3 47.14	48N15.69	114W 0.32	18.14	1.7	7	158	105.3	0.53	26.0	18.4	D
750123	1921 44.81	48N 9.16	114W 6.34	4.97	2.4	13	124	108.1	0.33	3.7	3.8	C
750124	1144 20.87	48N 9.67	114W 6.16	2.50	1.6	9	129	107.6	0.44	12.3	99.0	D
750125	130 2.86	48N 8.76	114W 4.32	0.63	1.8	10	131	110.4	0.30	4.2	99.0	C
750125	139 20.14	48N 8.37	114W 6.94	11.70	2.4	13	127	108.7	0.36	5.3	7.1	C
750131	854 45.87	48N 9.12	114W 6.77	13.09	3.8	16	119	107.8	0.34	3.3	3.2	C
750131	943 13.00	48N 8.14	114W 6.70	9.23	2.6	14	124	109.2	0.33	3.9	4.6	C
750131	1025 16.12	48N 9.86	114W 5.27	4.22	1.6	10	125	108.1	0.30	5.5	7.3	D
750131	1118 20.15	48N11.02	114W 2.34	2.50	1.9	10	188	117.0	0.21	4.7	99.0	D
750131	1124 21.75	48N 9.75	114W 5.77	2.50	1.7	9	130	107.8	0.17	5.1	48.9	C
750131	1148 14.12	48N 8.89	114W 5.60	0.31	2.0	12	127	109.1	0.28	3.8	99.0	C
750131	1310 33.40	48N 8.39	114W 7.54	2.50	2.0	11	125	108.1	0.29	3.7	53.2	C
750131	14 4 14.84	48N 9.35	114W 7.13	14.94	1.2	7	138	107.2	0.14	4.2	3.9	C
750131	14 9 7.52	48N 9.43	114W 5.21	2.50	1.9	7	128	108.7	0.29	13.1	99.0	D
750131	1751 38.67	48N 8.83	114W 5.36	3.17	2.5	11	125	109.4	0.29	3.9	7.0	C
750201	4 0 38.97	48N10.41	114W 3.74	11.39	1.7	10	130	108.7	0.25	5.4	4.3	C
750202	2 6 3.93	48N10.04	114W 4.86	10.57	2.7	10	126	114.3	0.16	2.4	2.8	B
750202	511 50.77	48N 8.31	114W 7.07	9.05	2.8	12	123	112.3	0.35	4.4	5.3	C
750202	654 22.41	48N 8.46	114W 6.35	11.59	2.5	12	123	113.1	0.43	5.1	5.5	D

750202	826	17.18	48N11.15	114W	2.14	9.98	1.7	8	139117.2	0.07	1.9	1.7	C
750202	1543	7.26	48N11.43	114W	1.46	13.97	1.8	8	147117.9	0.09	3.0	2.3	C
750203	420	21.82	48N 9.25	114W	6.60	7.65	2.1	11	121112.5	0.18	2.6	3.2	C
750203	729	15.85	48N 9.12	114W	3.60	2.50	2.0	10	134116.2	0.39	6.0	76.5	D
750204	132	58.12	48N 7.60	114W	10.05	14.63	5.0	14	175116.6	0.29	3.4	3.0	D
750204	2 7	32.03	48N 9.04	114W	5.36	9.05	2.1	13	125114.1	0.28	3.8	4.5	C
750204	226	46.57	48N10.21	114W	2.08	5.69	1.8	11	137117.6	0.47	5.1	9.4	D
750204	342	51.85	48N 9.36	114W	4.42	2.50	1.8	11	131115.1	0.34	4.9	63.2	C
750204	351	30.22	48N 8.18	114W	7.32	8.39	1.6	7	181146.0	0.11	4.3	4.0	D
750204	411	33.16	48N 8.76	114W	5.50	2.50	1.7	11	127120.6	0.19	2.0	26.8	C
750204	421	45.76	48N 9.44	114W	6.64	13.78	2.4	13	121112.4	0.32	3.8	3.6	C
750204	426	12.49	48N 9.25	114W	7.08	9.75	1.8	11	120111.9	0.37	5.2	6.1	D
750204	439	15.55	48N10.31	114W	3.34	2.50	1.5	5	191149.6	0.06	6.5	99.0	D
750204	5 5	13.32	48N 8.71	114W	6.11	2.50	2.4	11	125113.3	0.38	5.3	74.2	D
750204	5 9	6.54	48N11.63	114W	13.00	47.19	1.9	10	178153.2	0.37	9.1	99.0	D
750204	538	19.25	48N 8.84	114W	2.73	2.50	1.7	10	137117.3	0.72	10.4	99.0	D
750204	553	24.98	48N 8.47	114W	7.03	2.50	1.7	9	123112.3	0.20	2.7	37.0	C
750204	641	19.66	48N10.07	114W	3.58	8.70	1.7	8	138115.8	0.03	0.7	2.3	C
750204	1420	14.57	48N 9.99	114W	4.49	8.23	1.6	6	185149.0	0.08	4.4	4.1	D
750205	832	50.99	48N10.13	114W	2.62	9.69	1.6	10	137117.0	0.09	1.4	1.9	C
750205	1530	39.57	48N10.46	114W	2.48	2.50	1.8	7	192149.6	0.21	7.8	99.0	D
750205	1533	36.76	48N10.48	114W	3.77	12.94	1.5	7	191149.9	0.10	4.2	99.0	D
750205	1538	40.35	48N 7.92	114W	6.76	2.50	1.5	12	124112.9	0.34	4.1	64.1	C
750205	1539	42.44	48N 8.35	114W	6.02	2.50	1.9	12	126113.6	0.29	3.2	47.8	C
750210	2313	31.66	48N 8.84	114W	4.12	2.50	1.7	10	136115.7	0.23	4.0	43.3	C
750301	2320	8.95	48N 8.68	114W	7.08	2.50	1.6	11	122112.2	0.36	4.8	68.7	C
750301	2332	33.07	48N 8.35	114W	6.34	2.50	1.7	12	125113.2	0.31	3.6	53.4	C
750304	1242	46.62	48N 7.05	113W	54.48	0.63	2.0	8	166128.2	0.31	4.8	99.0	D
750314	818	20.01	48N 9.39	114W	4.98	2.50	1.6	10	133109.0	0.14	2.1	26.2	C
750402	436	34.91	48N 7.04	114W	11.34	2.50		10	180108.0	0.73	9.5	99.0	D
750402	1832	52.50	48N 9.22	114W	5.69	1.72		7	153108.6	0.66	32.3	99.0	D
750405	756	3.15	48N10.46	114W	6.03	1.25	1.5	8	128106.7	0.47	19.1	99.0	D
750405	942	7.44	48N 8.66	114W	4.94	2.70	2.3	12	127110.0	0.50	6.6	11.3	D
750408	1 0	6.58	48N 5.89	114W	9.98	1.05		7	133109.6	0.56	18.4	99.0	D

750409	2349	3.53	48N25.16	114W25.23	15.06		5	152	70.6	0.01	6.2	5.5	D
750417	1 4	40.52	48N10.47	114W 5.80	2.50	1.6	7	129	106.8	0.36	16.7	99.0	D
750426	857	52.61	48N 8.57	114W 6.81	0.63	1.7	8	128	108.5	0.48	8.1	99.0	D
750515	1229	24.73	48N 7.89	114W 7.91	0.63	1.7	13	125	108.5	0.35	3.5	99.0	C
750515	1231	0.22	48N 8.71	114W 6.36	4.71	2.1	17	122	108.7	0.45	5.1	6.9	C
750628	159	54.67	47N56.75	114W41.01	8.42	2.0	5	144	106.1	0.08	7.3	10.3	D
750702	2327	14.31	48N21.19	114W35.59	2.50		4	173	73.7	0.08	5.5	99.0	D
750829	1128	1.46	48N 9.46	114W 4.03	0.63		10	132	109.7	0.37	9.0	99.0	D
750908	1312	5.25	48N14.40	113W41.33	9.04	1.6	7	206	158.0	0.50	11.3	44.3	D
750917	1812	43.47	48N 6.97	114W18.61	35.85	1.3	7	171	108.1	0.22	9.3	18.2	D
751020	1417	53.38	48N 7.11	114W12.14	12.99	3.5	14	175	107.0	0.25	2.8	2.5	D
751028	0 9	19.96	48N18.33	113W45.45	1.25		6	207	188.2	0.53	42.8	99.0	D
751121	2249	58.92	48N 2.83	114W 8.70	1.10	1.8	15	183	115.0	0.40	5.9	4.3	D
760119	21 6	13.15	48N13.26	114W 1.46	13.90	1.8	14	148	107.2	0.47	6.3	4.5	D
760119	2250	36.87	48N 1.72	114W 1.52	10.02	1.6	10	142	122.4	0.48	13.8	42.4	D
760121	1343	30.26	48N 8.18	114W 7.31	5.41	3.2	11	120	108.6	0.30	4.2	6.9	C
760228	1023	42.04	48N22.04	114W14.77	1.21	2.1	9	191	99.4	0.36	10.7	9.4	D
760309	2347	54.99	48N12.29	114W 4.24	0.41		9	192	119.2	0.56	19.4	9.5	D
760320	714	11.37	48N 9.07	114W 9.41	0.31	2.1	18	119	105.7	0.46	4.1	5.4	C
760404	225	23.47	47N59.44	113W57.44	8.69		10	145	128.2	0.33	6.1	4.9	D
760407	134	40.35	47N 7.30	116W11.21	4.94	1.7	4	283	209.5	0.25	99.0	99.0	D
760424	320	33.59	48N10.50	114W 4.79	2.50	1.4	15	129	107.7	0.40	5.9	62.0	D
760424	325	34.50	48N10.34	114W 5.08	7.79	2.2	14	128	107.6	0.18	2.2	3.3	C
760424	841	23.15	48N 9.85	114W 6.77	0.53	2.5	12	122	106.8	0.13	1.8	99.0	C
760424	849	13.01	48N 8.22	114W 8.69	7.87	3.5	13	118	107.4	0.30	3.9	4.8	C
760424	1747	1.92	48N12.14	114W 3.01	0.63	2.4	13	189	115.8	0.42	6.3	4.1	D
760425	10 7	10.94	48N 8.13	114W 9.57	1.01	2.3	10	179	109.4	0.30	5.2	99.0	D
760520	2345	37.73	48N 7.01	114W12.38	0.63	1.4	5	176	169.3	0.49	14.9	99.0	D
760607	1728	14.04	48N 7.33	113W54.81	16.82	1.2	11	161	127.5	0.85	17.6	10.4	D
760811	1457	30.34	48N10.35	114W 7.97	2.50	2.5	14	117	105.1	0.51	5.5	82.3	D
761003	529	0.17	48N 8.58	114W 7.93	5.66	2.7	11	118	111.2	0.30	4.5	5.2	C
761003	555	50.51	48N10.15	114W 5.94	5.44	2.1	9	125	112.9	0.13	2.3	12.7	C

TABLE A3

DATE	ORIGIN	LAT N	LONG W	DEPTH	MAG	NO	GAP	DMIN	RMS	ERH	ERZ	Q
760819	4 1 17.55	48N10.04	114W 7.20	10.38		10	97	8.8	0.13	1.0	2.1	B
760819	752 12.25	48N 9.95	114W 7.23	9.80		10	96	8.8	0.10	0.8	1.8	B
760819	759 28.10	48N 9.86	114W 6.62	10.46		10	90	9.6	0.18	1.4	2.9	B
760819	822 1.86	48N10.25	114W 7.22	9.50		8	162	10.6	0.08	1.1	1.9	C
760819	840 55.08	48N 9.84	114W 7.40	9.58		8	159	10.0	0.06	0.9	1.5	B
790814	1756 45.24	48N 1.10	114W 8.62	11.04		7	276	21.1	0.07	2.1	1.5	C
790816	19 8 32.63	48N 3.08	113W59.21	1.82		8	287	20.5	0.17	3.5	13.9	D
790820	947 28.70	48N11.59	114W 5.83	10.52		6	219	6.5	0.03	1.0	1.1	C
790821	1224 55.64	48N 3.78	114W 6.72	11.34		9	253	15.6	0.08	2.7	3.1	C
790824	5 6 31.51	48N11.13	114W15.04	11.47		12	170	13.4	0.09	0.8	1.3	B
790830	337 19.90	48N19.94	114W 4.50	0.67		9	295	19.8	0.11	2.4	43.6	D
790901	1358 14.32	48N17.97	114W21.45	10.52		9	298	23.1	0.19	4.8	7.5	D
790902	1851 16.28	48N11.56	114W 5.62	13.63		9	193	14.0	0.08	1.8	1.4	C
790910	453 19.11	48N 6.23	114W 7.89	7.53		12	115	12.8	0.17	1.4	2.6	B